2010

Desulfurization and tar removal from gasifier effluents using mixed rare earth oxides

Sumana Adusumilli
Louisiana State University and Agricultural and Mechanical College, sadusu1@lsu.edu

DESULFURIZATION AND TAR REMOVAL FROM GASIFIER EFFLUENTS USING MIXED RARE EARTH OXIDES

A Thesis

Submitted to the Graduate Faculty of the
Louisiana State University and
Agricultural and Mechanical College
in partial fulfillment of the
requirements for the degree of
Master of Science in Chemical Engineering

In

The Department of Chemical Engineering

By
Sumana Adusumilli
B.Tech., Andhra University, 2007
May 2010

ACKNOWLEDGEMENTS

First and foremost I would like to thank my parents for their love and support. I would like to thank my advisor Dr. Kerry M. Dooley for his guidance, encouragement and support through out my research work. I would like to thank my committee Dr. Gregory L. Griffin and Dr. John Flake for their invaluable suggestions. I would like to thank Dr. Amitava Roy for helping me with the XRDs. I would like to thank Vikram Kalakota, Bobby Forest and Cassidy Sillars for helping me in the lab. My thanks to Melanie and Darla for helping me with my administrative requirements. Finally, I would like to thank all my classmates and friends at LSU for making my life easy.

TABLE OF CONTENTS

LIST OF TABLES

LIST OF FIGURES

ABSTRACT

Biomass gasification is a promising source of fuels. However, hydrogen sulphide, tars and other by-products must be removed from the raw gas because they deactivate downstream reforming and water gas shift catalysts. The goal of this project is to find the best REO combination for simultaneous tar cracking and desulfurization of gasifier effluents and to find the sorbents that are stable at high operating temperatures of gasifiers. Simultaneous tar cracking and H_2S removal from a simulated gasifier effluent was tested using different rare earth mixed oxide (REO) catalysts/sorbents based on Ce/LaO_x, $Ce/La/MO_x$ and $Ce/La/M_2O_x/Al_2O_3$ where M is a transition metal and M_2 is a third rare earth metal. These catalysts were prepared using sol gel and incipient wetness impregnation methods. Desulfurization tests were done at 903K using a gas composition of 23.4% H_2, 32% CO_2, 3.1% H_2O, 41.4% N_2 and 0.1% H_2S. The tar cracking/reforming capability of these materials was tested by adding 0.35 mole% naphthalene as a model compound of tar to the simulated effluent and reacting it during the adsorption cycle.

Sorbents containing pure Ce/La oxides have low sulfur capacities and are not very effective in removing H_2S from a real gasifier effluent. Supporting the REOs on Al_2O_3 (20 wt% REO) or ZrO_2, and addition of a small amount of a third REO known to enhance the thermal stability of CeO_2 (either Tb_2O_3 or Gd_2O_3), greatly increased the total sulfur capacities of the REOs. These ternary REOs maintained their capacity over a minimum of four successive runs and were regenerated in air. The tar removal capacity of these sorbents was found to be low in the simultaneous presence of H_2S, H_2O and CO_2 and all the sorbents deactivated in 30 mins. A mixed Ce/La/Mn oxide was found to be the best catalyst for simultaneous desulfurization and tar removal.

CHAPTER 1

INTRODUCTION AND REVIEW OF LITERATURE

1.1 Biomass Gasification

Biomass gasification involves the partial combustion of biomass to produce gaseous fuels by heating in (typically) air, oxygen, steam, or steam-oxygen mixtures. The product gas contains ash particles, volatile alkali metals and tars as well as synthesis gas. "Tar" is a generic term comprising all organic compounds in the product gas excluding C1-C6 gaseous hydrocarbons (Neeft et al., 2002). Others define tars as any hydrocarbon >C2. The gaseous fuels must be cleaned of tars and particulates. Tars can cause several problems, for example coke formation in the pores of filters, plugging the filters (Aznar et al., 1998).

Biomass feedstocks primarily consist of forest and agricultural residues, urban wood wastes and dedicated energy crops (Torres et al., 2007). The feedstocks are of two general types, cellulosic biomass and proteinaceous biomass. The gas yield after conversion of the protein-containing biomass is often low and severe corrosion has been observed in hydrothermal gasification of protein-containing biomass (Kruse et al., 2005).

Different types of cellulosic biomass have been used to study biomass gasification, including pine wood chips (Aznar et al.,1998), poplar wood (Arauzo et al., 1997), pine sawdust (Garcia et al., 2002), cedar wood (Asadullah et al., 2003), wood sawdust (Waldner et al., 2005), Radiata pine (Tasaka et al., 2007), bagasse (Turn 2007), grass silage (Schmersahlet al., 2007), almond shells (Rapagna et al., 1998), and cattle manure (Schmersahl et al., 2007; Elliott et al., 2004). The biomass is a mixture of different compounds varying in composition. A typical wood contains 3 wt% extractives, 23-35 wt% lignin, 20-22 wt% hemicellulose, and 43-49 wt%

cellulose. Since feeding a real biomass on a laboratory scale is difficult, and because understanding the chemistry of a pure component is easier than understanding that of a mixture, many different model compounds have been used to study gasification (Kruse et al., 2005). Cellulose (Dalai et al., 2003, Asadullah., 2002, Fushimi et al 2003), lignin (Fushimi et al., 2003), and glucose (Kruse et al., 2005) have all been used as model compounds for biomass. The elemental feed composition of biomass for a typical gasification process in wt% is: carbon, 49-52%; hydrogen, 5-7%; nitrogen 0.1-2%; oxygen, 40-43%; sulfur, 0.02-0.3%; chlorine < 0.1% (Pengmei et al., 2007; Zhang et al., 2005; Juutilainen et al., 2006; Arauzo et al., 1994).

The composition of the gas at the exit of a gasifier depends mainly on the type of biomass feed, biomass feeding rate, type of gasifier, gasifying agent (reactant), gasifying agent/biomass ratio, gasifier bed temperature and heating rate (Caballero et al., 1997; Kruse et al., 2005; Asadullah et al., 2002, Fushimi et al., 2003). Because alkali salts catalyze the water-gas shift reaction, the hydrogen yield from biomass gasification is positively affected by a high content of alkali salts in biomasss (Kruse et al., 2000). High lignin content adversely affects hydrogen production (Schmeider et al., 2000). High gasifier temperatures result in less tar (Kinoshita et al., 1994; Corella et al., 1999). Increasing the gasifier temperature to 1000-1200 K decreases the tar formation by 35% (Ferreira- Aparicio et al., 2005). The temperature range around 1100 K is favorable for gasification of several types of biomass (Milne et al., 2003)

Different gasifying agents (reactants) such as air, steam, steam-oxygen and carbon dioxide have been used. The product gas composition from the gasification of pine wood chips using air at 1053-1113 K with equivalence ratio (ER, the ratio of actual air to fuel ratio to air to fuel ratio required for complete combustion) 0.18-0.45 is 5-16 vol% H_2, 10-22% CO, 9-19% CO_2, 2-6% CH_4, 42-62% N_2, 11-34% H_2O, and 0-3% C_2 fraction (Gil et al., 1999). The product

gas composition from the gasification of pine wood chips using steam at 1023-1053 K was 38-56 vol% H_2, 17-32% CO, 13-17% CO_2, 7-12% CH_4, 52-60% H_2O, and 2% C_2 fraction (Gil et al., 1999). Tar content sharply decreases as ER increases. Higher ER values decrease H_2 and CO concentration in the product gas (Narvaez et al., 1996). At 823 K, only 53% of the carbon was converted in the gasification of cellulose by air. Both CO and H_2 were hardly formed. But by using a Rh/CeO_2 gasification catalyst, 100% carbon conversion was achieved. Ceria itself has catalytic activity in the production of syngas (Asadullah et al., 2001).

Typical reactions proposed for cellulose gasification by air are (Asadullah et al., 2001):

$$\text{Cellulose} \rightarrow CO_2 + H_2O$$

$$\text{Cellulose} \rightarrow CO + H_2O$$

$$\text{Cellulose} \rightarrow \text{Tar} + H_2O$$

$$\text{Tar} + H_2O \rightarrow CO + H_2 \ (H_2/CO > 1)$$

$$\text{Tar} + O_2 \rightarrow CO_2 + H_2O$$

$$CO + H_2O \rightarrow CO_2 + H_2$$

$$CO + 3H_2 \rightarrow CH_4 + H_2O$$

Higher heating rates increase the final conversion of biomass and decrease char production in steam gasification (Fushimiet al., 2003). Increased heating rates significantly increased CO, H_2, and CH_4 yields in the steam gasification of biomass (Fushimi et al., 2003). Proposed reactions in the steam gasification of biomass are (Raman et al., 1980; Cs represents the carbons in cellulose):

$$Cs + \text{Heat} \rightarrow CO + CO_2 + CH_4 + \text{other hydrocarbons} + \text{organics} + \text{oxygenated compounds} + \text{charcoal}$$

Or if the temperature is sufficiently high, additional reactions take place:

$$CH_4 + H_2O \rightarrow CO + 3H_2$$

$$CH_4 + CO_2 \rightarrow 2\,CO + 2H_2$$

$$CO + H_2O \rightarrow CO_2 + H_2$$

$$C + CO_2 \rightarrow 2CO$$

At temperatures above 973K, the following reactions were proposed:

$$Cs + H_2O \rightarrow CO + H_2$$

$$Cs + 2H_2O \rightarrow CO_2 + 2H_2$$

$$2\,C_S + 2\,H_2O \rightarrow CH_4 + CO_2$$

$$Cs + CO_2 \rightarrow 2\,CO$$

Catalytic steam gasification of almond shells using steam reforming nickel catalysts at 1103 K, GHSV 1800h^{-1}, and biomass to steam ratio 1 gives a gas composition of H_2 - 62.1 mol%, CO - 22.7, CO_2 - 15.7%. The gas yield was 1.98 m^3/kg of biomass and the tar yield was 0.23 g/m^3; without a catalyst the gas was 1 m^3/kg of biomass and the tar 100 g/m^3, at 1043 K(Fushimi et al., 2003). Steam reacts with char above 773 K and does not affect the tar evolution in the low temperature (600-700 K) pyrolysis region. This suggests that pyrolysis is an initial stage of steam gasification (Fushimi et al., 2003).

Pyrolysis at higher temperatures (ca. 773K) can convert biomass to vapors, gases and charcoal in the absence of oxygen. At lower temperatures (673 K), the pyrolysis gas contained mainly CO_2 and CO. Formation of H_2 was less than 2% of CO_2 and formation of CH_4, C_2H_4 and

C_2H_6 was negligible (Yamaguchi et al., 2006). At 600-700K, 81% of the cellulose converts into tar, also evolving CO_2, CO and H_2. (Fushimi et al., 2003).

The product gas composition from the gasification of pine wood chips using both steam and O_2 at 1058-1113 K with ER 0.24-0.51 is 14-32 vol% H_2, 43-52% CO, 14-36% CO_2, 6-8% CH_4, 38-61% H_2O, 3-4% C_2 fraction (Gil et al., 1999). The gas efficiency of air gasification is 35-70% (Gil et al., 1999), while that of steam - oxygen gasification is about 70% (Caballero et al., 1997). CO_2 gasification in the presence of a Ni/Al catalyst transforms tars, decreases the amounts of CH_4 and C_2 fraction, and increases H_2 and CO yields (Garcia et al., 2000), but the catalyst deactivates rapidly.

Wet biomass contains up to 95% water and results in high drying costs if conventional gasification is used. Hydrothermal gasification is an alternative, either near or above the critical point of water (647 K, 22.1 MPa). The product gas composition from hydrothermal gasification of wood sawdust at 683 K, 29.3 MPa is CO – 9 mol%, H_2 - 16%, CH_4 - 14%, CO_2 - 61%. The carbon gasification efficiency was only 21%. By using a Raney nickel catalyst at 573-683 K and 12-34 MPa, the carbon gasification efficiency was increased to 77-100%. The gas contained 23-48 mol% CH_4, 43-59% CO_2, 3-24% H_2 and <0.1% CO. At supercritical conditions, the liquid phase was tar free and contained less that 2% of the feed carbon (Waldner et al., 2005). H_2 and CO_2 formation increased at higher water content; CH_4 formation increased at lower water content (Kruse and Gawlik 2003). An increase in temperature led to an increase in the gasification efficiency. Above the critical temperature of water, a drastic increase in the yields of H_2 and CH_4 and a decrease in CO were found. The pressure dependence of gas formation was only relevant above the critical point of water, where yields of H_2 and CO_2 decreased and the yield of C_2's increased with pressure (Kruse and Gawlik 2003).

Biomass, depending on its type, may contain a variety of downstream catalyst poisons, such as sulphur, chlorine and alkaline metals. For example, sewage sludge contains a large amount of sulphur and thus the product gas contains hydrogen sulphide, carbonyl sulphide and sulphur dioxide in high concentrations (Hepola and Simell ., 1997). The product gas composition from gasification of dried sewage sludge in a fluidized bed gasifier containing dolomite and using air and steam at 1123-1173 K is 12-14 vol% H_2, 7-8% CO, 2-3% CH_4, 1-2% C_2H_4, 16-18% CO_2, 55-60% N_2, 18-22% H_2O, 2-5g/m^3tar, <100 ppm H_2S, <200 ppm SO_x, <10 ppm COS (Sato and Shinoda., 2007).

1.2 Biomass Gasifier Catalysts and Their Effects on Product Gas Compositions

For combustion in most engines, the tar content in fuel gases must be lower than 10 mg/m^3 (Bui et al., 1994). The homogeneous destruction of tars by cracking takes place above 1123 K (Kinoshita et al., 1994). Tar removal from a gasifier product is typically by either or both of two methods: hot gas cleaning after the gasifier ("secondary" method), and treatment inside the gasifier ("primary" method). Increasing the temperature usually decreases the tar content in the product gas. Other operating parameters in the gasifier such as gas reactant, equivalence ratio, residence time etc. also affect the formation and composition of tar. Residual tars can be decomposed by both steam and dry (CO_2) reforming reactions. Adsorption of tar on the catalyst surface is often the rate determining step of biomass tar decomposition, and catalysts with larger surface areas exhibit higher conversions of tars (Tasaka et al., 2007).

A typical composition of biomass tars in wt% is: toluene - 24%; other one ring aromatic hydrocarbons - 22%; naphthalene - 16%; other two ring aromatic hydrocarbons - 13%; three ring aromatics - 6%; four ring aromatic hydrocarons-1%; phenolic compounds - 7%; heterocyclic compounds - 10%; others - 2% (Coll et al., 2001). Tasaka et al. (2007) compared tar obtained

from steam gasification of cellulose and steam gasification of real biomass. In steam gasification of cellulose, using a 12% Co/MgO catalyst, all the recovered tar was water soluble. In steam gasification of Radiata pine with the same catalyst, the water soluble tar was only 52%. The different tendencies for tar production and conversion have been attributed to different phases of tar in contact with the catalyst: liquid /solid for cellulose tar, but gas/solid for biomass tar.

Biomass gasifier catalysts (when used) are mainly calcined rocks (e.g., olivine), clay minerals, alkali or alkaline earth oxides, or ferrous metal oxides. All such catalysts affect the gas composition, both decreasing the amount of tars and CO, and increasing H_2 and CO_2 (Caballero et al., 1997). To prevent deactivation of downstream nickel steam reforming catalysts, the tar content of the product gas should be less than 2 g/m^3. This can sometimes be achieved with dolomite, which decomposes "soft" tars such as phenol derivatives (Cabarello et al., 1997), but not refractive tars such as PAHs, which may actually increase (Narvaez et al., 1997). The most commonly used primary (in the biomass bed) catalytic materials are dolomites, olivines and other calcined minerals (Cabarello et al., 1997; Mastellone and Arena 2008). These all can reduce the amount of tar in the effluent.

Simell et al. (1992) classified calcined minerals according to CaO/MgO ratio. The catalytic activity of such minerals for tar elimination is due to their high alkali (K, Na) content. The activity of these rocks can also be improved by increasing the Ca/Mg ratio, decreasing the grain size, and increasing the content of an active metal such as iron (Simell et al., 1992).

Olivine [$(Mg,Fe)_2SiO_4$] has a higher attrition resistance than dolomite (Rapagna et al., 2000), but its catalytic activity for tar decomposition is lower (Courson et al., 2000). At 1023 K, olivine intercalated with a small amount of Ni^{2+} has a high activity for dry reforming (95% methane conversion) and steam reforming (88% methane conversion) (Courson et al., 2000).

Clay minerals belong to the kaolinite, montmorillonite and illite groups (El Rub et al., 2004).The catalytic activity for tar elimination of these clay minerals depends upon the effective pore diameter, surface area and number of acidic sites (Wen and Cain1984). They typically have lower gasification activity compared to dolomite and cannot be used at temperatures >1070 K (Simell and Bredenberg., 1990).

Metallic iron can also catalyze tar decomposition, more effectively than the oxides. Iron also catalyzes the water-gas shift reaction (Simell et al., 1992); but the activities of magnetite (Fe_3O_4) and hematite (Fe_2O_3) catalysts for the decomposition of tarry compounds in fuel gas in the temperature range of 973K – 1173K were lower than that of of dolomite. For steam gasification of cellulose using a primary Co catalyst at 873 K, tar conversion increased with Co loading. A 36 wt% Co/MgO catalyst showed 84% tar conversion and 67% carbon conversion to gas. The amount of recovered tar and the elemental composition of the recovered tar was independent of S/C ratio (Tasaka et al., 2007).

1.3 Tar Cracking of Gasifier Effluent

Different model tar compounds have been used to study the "secondary" tar cracking of simulated gasifier effluent. Naphthalene (Furusawa and Tsutsumi 2005; Nacken et al., 2007; Sata and Fujimoto 2007; Bampenrat et al., 2008), toluene (Pansare et al., 2008; Lamacz et al., 2009; Juutilainen et al., 2006), and benzene (Nacken et al.,2007; Furusawa et al 2009) have all been used.

In secondary steam reforming of tar derived from cellulose gasification using 12 wt% Co/MgO (873 K, S/C 0.6-1.3, 0.06 s residence time), 80% of the tars were converted. For steam reforming using a simulated gas containing 3.5 mole% naphthalene, 21 mole% H_2O, 20 mole%

N_2, and 55.5 mole% Ar, using a 12% Co/MgO catalyst, (1173 K, GHSV 3000h^{-1}, S/C ratio 0.6), 23% of the carbon was converted to gas with a final gas composition of 70% H_2, 27.5% CO_2, 2.4% CO, 0.1% CH_4. The catalytic activity of this Co/MgO was greater than that of Ni/MgO (Furusawa and Tsutsumi ., 2005). In later work, Tasaka et al. (2007) tested Co/MgO catalysts with different Co loadings. Catalysts with larger surface area exhibited higer conversion for tar cracking of an actual steam gasifier effluent at 873K. Sato and Fujimoto (2007) reported that a Ni/MgO-CaO catalyst doped with WO_3 as a sulphur-resistant promoter also showed high naphthalene reforming activity, and was stable in gas containing 300 ppm H_2S at 1073 K, GHSV 14,000h^{-1}.

Complete conversion of naphthalene was obtained with Ni/Al_2O_3 catalysts doped with MgO, using a H_2S-free synthetic fuel. However, naphthalene conversion decreased below 30% in gasification with a synthetic fuel containing 200 ppm of H_2S at 1023K and having a face velocity of 2.5 cm/s (Ma et al., 2005). A Ni/Olivine catalyst contacted with 87.75 vol% Ar, 11.6% H_2O, and 0.7% toluene at 923 K, 3 NL/h gave complete toluene conversion to syngas. However, the product from steam reforming of toluene on just olivine contained polyaromatics (14%), benzene (6%) and methane (2%), formed from CO, CO_2, and H_2. The conversion of toluene was only 37% (Swierczynski et al., 2006). Hepola and Simell (1997) also found that the tar cracking activity of Ni-based catalysts decreased as a result of H_2S adsorption, whereas ammonia conversion was enhanced by a higher H_2S concentration. High operating temperatures lessened the catalyst deactivation caused by the H_2S (Hepola and Simell 1997).

Nickel-based tar cracking catalysts are generally placed downstream of the gasifier (Corella et al., 1997). When using typical naphtha steam reforming catalysts, the H_2 and CO

contents increase somewhat, while CH_4 decreases by 0.5 -2.5 vol%, and C_2H_n by 1-1.8 vol% (Caballero et al., 2000).

1.4 Catalyst Life

Long term tests – hundreds of hours - are needed to check the feasibility of the tar cracking catalysts at a commercial scale (Aznar et al., 1998). For commercial steam reforming Ni-based catalysts at 1100 K, there was no deactivation for 45 h on stream in the steam gasification of pine wood chips (Aznar et al., 1998). A MgO-supported Ni catalyst (6% Ni) was active for naphthalene reforming (Nacken et al., 2007). A model gas containing 50% N_2, 12% CO, 10% H_2, 11% CO_2, 5% CH_4, 12%H_2O, 0.0875% naphthalene, and 100 ppmv H_2S was used at GHSV 2080 h^{-1} and at 1073K. Complete naphthalene conversion was achieved even after 100 h operation.

1.5 Mn- and V-Containing Sorbents for Desulfurization

Removal of sulfur from the gases exiting the gasifier is necessary as it poisons water-gas shift catalysts and poses environmental problems. Mixed oxides based on Zn, Fe and Ti showed good performance for desulfurization, but at high temperatures they were reduced to the metallic state (Desai et al., 1990). Of all the different inorganic oxides tested, MnO exhibited the highest initial reaction rate with H_2S in the temperature range 573- 1073 K (Westmoreland et al., 1977). MnO is the stable phase prior to sulfidation in this temperature range, and Mn-based sorbents are not reduced to metallic state at high temperatures.

Manganese oxides do not exhibit favourable sulfidation thermodynamics compared to ZnO. But the rate of sulfidation of Mn oxide sorbents was substantially higher than that exhibited

by conventional ZnO-based sorbents (Ben-Slimane and Hepworth 1994). Sulfidation of Mn-based sorbents is high at 1073-1173 K.

The reactions taking place during reduction, sulfidation and regeneration of Mn-based sorbents are (Alonso and Palacios 2002):

$$Mn_3O_4 + H_2 \rightarrow 3MnO + H_2O$$

$$MnO + H_2S \rightarrow MnS + H_2O$$

Regeneration (using air)

$$3MnS + 5O_2 \rightarrow Mn_3O_4 + 3\ SO_2$$

$$MnS + 2O_2 \rightarrow MnSO_4$$

$$3\ MnSO_4 \rightarrow Mn_3O_4 + 3\ SO_2 + O_2$$

Natural manganese ore consisting mainly of β-MnO_2 is a potential sorbent catalyst for the simultaneous removal of SO_x/NO_x. The main product is β-$MnSO_4$. In order to maintain the removal efficiency of SO_2 and NO above 80% and the concentration of NH_3 in the effluent gas below 5 ppm, the reaction temperature and residence time of the ore was controlled at 623 – 673 K and less than 30 min. The surface area of the sorbent decreased due to formation of $MnSO_4$, which plugged the pores, decreasing the capacity for SO_2 (Jeong et al., 2001). The addition of CuO and NiO to the ore resulted in a shorter reduction time and higher sulfidation capacity (Yoon et al., 2003).

Manganese-based sorbents doped with different concentrations of copper showed increased reactivity and stability of the copper oxide, but still thermal sintering (Alonso et al., 1999; Garcia et al., 2000). Sulfidation at 973 K on Mn-CuO_x with a gas composed of 0.5 vol%

H_2S, 10% H2 and balance N_2 gave a pre-breakthrough H_2S concentration below 50 ppmv. The presence of Cu in the Mn-based sorbents was necessary to lower the H_2S concentration to sub ppm levels (Garcia et al., 2000). For MnO doped with ZnO some decay in capacity was observed in 70 sulfidation – regeneration cylces. Sulfidation tests done at 973 K using a gas containing 1 vol% H_2S, 10% H_2, 15% H_2O, 5% CO_2, 15% CO and balance N_2 gave a pre- breakthrough H_2S conc. of 10–15 ppmv. Regeneration was with pure air at 1073 K (Alonso and Palacios 2002).

An 8% MnO/γ-Al_2O_3 is a regenerable sorbent for the removal of H_2S (Atakul et al., 1995):

$$MnO / \gamma\text{-}Al_2O_3 + H_2S \leftrightarrow MnS / \gamma\text{-}Al_2O_3 + H_2O.$$

The active compound in this reaction may be $MnAl_2O_4$. The sulfide can be regenerated by steam (Wakker et al 1993). A higher temperature than 873 K increases the breakthrough capacity, but also the deactivation due to sintering. The breakthrough and total capacity of the sorbent were affected by both flow rate and H_2S concentration, the breakthrough capacity decreasing as the flow rate increased. Mn conversion ranged form 15-19% at breakthrough to 32-35% at maximum sulfidation. The sorbent was completely regenerated at 873 K using N_2/H_2/steam mixtures. Thermodynamic calculations show that acceptors with higher manganese content have higher sulfur capacity. Bakker et al., (1996) achieved 17 wt % sulfur capacity with a 32 wt % Mn sorbent. But it could not be easily regenerated. Repeated impregnations of small amounts of Mn gave a high Mn dispersion on alumina, which resulted in high capacity. When the Mn content was increased to 35 wt%, a sulfur capacity of 22 wt % of sulfur was obtained (Liang et al., 1999) at 1123 K for 50% H_2, 1% H_2S in Ar. Regeneration was at 1123 K using 30% H_2O in Ar. No deactivation was observed in 11 sulfidation –regeneration cycles. Another sorbent containing MnO, $MnAl_2O_4$ and Mn-Al-O phases showed a sulfur capacity of 20 wt% S, and was stable during 110 sulfidation- regeneration cycles (Bakker et al., 2003). Both MnO and

$MnAl_2O_4$ adsorb H_2S, but MnO adsorbs H_2S and COS more strongly. MnO adsorbs H_2S better than $MnAl_2O_4$ in the presence of water (Bakker et al., 2003).

Carbonyl sulfide (COS) is formed by the reaction of CO and H_2S:

$$CO + H_2S \leftrightarrow H_2 + COS$$

COS is not formed until after H_2S breakthrough (Wakker et al., 1993), and it increases with high carbon monoxide and low hydrogen concentrations. COS may be removed by direct reaction with the sorbent or it may be converted to H_2S. In the presence of H_2 and H_2O, COS is converted to H_2S as follows:

$$COS + H_2O \leftrightarrow H_2S + CO_2$$

$$COS + H_2 \leftrightarrow H_2S + CO$$

COS reacts with the acceptor as follows:

$$COS + MnO/\ \gamma\text{-}Al_2O_3 \leftrightarrow\ MnS/\ \gamma\ –Al_2O_3 + CO_2$$

Thermodynamics show that this reaction is favourable at 600-1100 K.

Vanadium-based mixed oxides can oxidize adsorbed H_2S to sulfur. Among the mixed oxides tested (V/Mo, V/Bi, V/Mg), V/Bi gave the highest sulfur yield. The maximum sulfur yield (97%) was higher than that obtained with vanadium oxide (78%, Li et al., 1996). The reactions taking place in the oxidation of H_2S are (Terorde et al., 1993):

$$H_2S + ½\ O_2 \rightarrow (1/n)\ S_n + H_2O\ (n=6\text{-}8)$$

Side reactions:

$$H_2S + 3/2\ O_2 \rightarrow SO_2 + H_2O$$

$$(1/n)\ S_n + O_2 \rightarrow SO_2$$

$$(3/n)\ S_n + 2H_2O \leftrightarrow H_2S + SO_2$$

The catalytic performance of the rare earth orthovanadates $REVO_4$ (RE = Ce, Y, La, Sm) was superior to that of MgV_2O_6, the sulfur yield decreasing in the order $CeVO_4$> YVO_4> $SmVO_4$> $LaVO_4$. Sulfur yields of both $REVO_4$ and MgV_2O_6 were much better than those of corresponding single oxides. Temperature programmed reduction showed that the reduction of V cations in $REVO_4$ was more difficult than in vanadium oxide. XRD measurements indicated the bulk structures of $REVO_4$ and magnesium vanadates were more stable than vanadium oxide (Li and Chi, 2001).

1.6 Regeneration Strategies for Mn-Based Sorbents

Manganese based sorbents can be regenerated using air, steam, SO_2 or an SO_2/O_2 mixture. In contrast, Zn-based sorbents cannot be regenerated using air (Ben-Slimane and Hepworth 1994). The main problem in regenerating Mn-based sorbents is the formation of $MnSO_4$, which decreases the capacity of the sorbents in the long run. In oxidative regeneration, $MnSO_4$ becomes unstable above 1073 K (Ben-Slimane and Hepworth 1994), and is not formed at 1173K. Both the rate of sulfidation and the thermal sintering are not greatly affected by the operating temperature of the sorbent (Garcia et al., 2000).

Steam regeneration can prevent the formation of $MnSO_4$ and also prevent hot spots. But steam regeneration cannot replace completely the oxidative regeneration process, because it is slow and usually incomplete. Regeneration using steam is also two times slower than SO_2 regeneration (Atakul et al., 1996). The following reactions take place with steam and SO_2, respectively:

$$MnS + H_2O \leftrightarrow MnO + H_2S$$

$$MnS + \tfrac{1}{2} SO_2 \leftrightarrow MnO + 0.75\ S_2$$

For ZnO-doped MnO, $MnSO_4$ was formed during the first stages of regeneration, but it decomposed in the last stages of the process (Alonso and Palacios 2002). Sulfided $MnAl_2O_4$ can be regenerated using with either SO_2 or H_2O leading to elemental sulfur or H_2S. For MnS/Al_2O_3, direct regeneration with SO_2 at above 700 K is possible without sulfate formation (Bakker et al., 2003). But regeneration with H_2O or SO_2 usually requires a lot of regeneration gas.

1.7 Rare Earth Oxides (REOs) for Desulfurization and Tar Cracking

While Ni (on Al_2O_3, e.g.) can crack tars to CH_4 and CO_x at 1100 K, there is rapid coking of the catalyst. However, Ni promoted by CeO_2 shows improved coking resistance (Devi et al., 2003). Similarly, a MgO or basic oxide-doped Al_2O_3 support also reduces deactivation of Ni-based catalysts by carbon deposition (Bangala et al., 1997).

Among a wide range of metal oxides, CeO_2 was reported to have excellent activity for the oxidation of naphthalene and a high naphthalene adsorption capacity (Garcia et al., 2006). But the problem with CeO_2 as a sulphur adsorbent is its slow adsorption, related to slow redox kinetics (Colon et al., 1998; Flytzani-Stephanopoulos et al., 2006). The reducibility of CeO_2 can be enhanced if intimately mixed with certain other oxides. Substitution of Ce^{4+} with Zr^{4+} in the CeO_2 lattice improves the oxygen storage capacity, redox properties and thermal resistance. CeO_2 films can be completely reduced at 900 K when supported on YSZ (yttria-stabilized ZrO_2), and the process is reversible even at higher temperatures (Costa - Nunes et al., 2005). High oxygen mobility and oxygen storage capacity make CeO_2/ZrO_2 a good catalyst for reforming reactions (Pengpanich et al., 2002; Pengpanich et al. 2006).

CeO_2-ZrO_2 mixed oxide catalysts showed good activity for the oxidation of naphthalene (Bampenrat et al., 2008). The extent of activity was related to the reducibility. $Ce_{0.75}Zr_{0.25}O_2$ showed a high selectivity to CO_2 in the oxidation of naphthalene (Bampenrat et al., 2008). Another benefit of Ce/Zr oxides is their resistance to carbon deposition (Lamacz et al., 2008). A $Ni/CeO_2/ZrO_2$ catalyst was also found to be promising for steam reforming of tar (Lamacz et al., 2008). Such catalysts have also exhibited good resistance to carbon deposition and high activity for the steam reforming of methane (Ramirez- Cabrera et al., 2003). A Zr/Al_2O_3 also shows good activity in the oxidation of tar and ammonia in a biomass gasifier effluent, at low temperatures (below 873K). The presence of H_2S had little effect on this catalyst (Juutilainen et al., 2006).

1.8 Motivation for this Work

It is hypothesized that mixed REOs (e.g., $CeO_2/La_2O_3/Tb_2O_3$) could simultaneously adsorb H_2S (to give M_2O_2S), crack tars and reform slip methane. The oxides can be regenerated with O_2 at ~900 K (Zeng et al., 1999). For 10-30 at.% La with CeO_2, the rate constant for the reduction of CeO_2 increases by more than ten times, with reduction substantial at 1070 K (Loong et al., 1999; Bernal et al., 1998). Mixtures of CeO_2 with La are not long-term stable under reducing conditions at >1200 K (Bernal et al., 1998). While CeO_2/La_2O_3 is an effective H_2S sorbent at >873 K, at least initially, it rapidly loses surface area and so sulfur adsorption capacity (>80% after 3 redox cycles, Wang et al., 2005). However, Gd_2O_3, Tb_2O_3 and Sm_2O_3 dopants similarly increase the rate of reduction (Huang et al., 2005; Bernal et al., 2002), and there are indications that these oxides can thermally stabilize CeO_2/La_2O_3.

Another problem with CeO_2 is the formation of sulfate during oxidative regeneration. While this problem may be alleviated by operating at high space velocities and low sorbent loadings, such conditions are not practical for long-term operation (Flytzani-Stephanopoulos et

al., 2006). Therefore more stable mixed REOs that are active for hot gas cleanup, tar cracking, and as reforming catalysts are needed. It is the purpose of this thesis to explore mixed REOs for these uses. They will be used either as neat mesoporous oxides, or supported on Al_2O_3, or impregnated with an added transition metal oxide (MnO) to further enhance the kinetics of sulfidation.

While it is not necessary to depart entirely from CeO_2 in order to obtain an oxide mixture active for desulfurization, other REOs are clearly necessary. The mixed CeO_2 phase should also be more active for tar cracking and further reforming of slip methane than other single REOs such as La_2O_3, because of the excellent redox behaviour of CeO_2. Supported (on Al_2O_3) mixtures of CeO_2/La_2O_3/third REO may prove superior to the mixed oxides alone, because Al_2O_3 can better stabilize (less crystalline ripening) the mixed REO phase when local hot spots occur during regeneration. The goal is to find the best REO combination for simultaneous desulfurization and tar removal from gasifier effluent streams.

CHAPTER 2

EXPERIMENTAL

The oxide sorbents/catalysts used here were prepared by either sol-gel (SG) or incipient wetness impregnation methods (IWI).

2.1 Sol –Gel Method

Measured amounts of cerium precursor ceric (IV) ammonium nitrate $(NH_4)_2Ce(NO_3)_6$ (Aldrich 99.9%; FW = 548.25) and lanthanum precursor La nitrate $La(NO_3)_3$*6 H_2O (Alfa Aesar 99.9%; FW = 433.1) salts were added to measured amounts of water and TMAOH surfactant with stirring. The salts dissolved immediately, forming a clear solution. To this solution $NH_4(OH)$ (Alfa Aesar, 28-30% NH_3) was added slowly until precipitation occurred (pH ~10.5). The temperature was raised to 363 K and the suspension stirred for 4 days. Every day the pH was checked and brought back to the precipitation pH by adding $NH_4(OH)$. Finally, the precipitate was separated using a centrifuge. The solids were washed with deionised water, acetone, then deionised water, dried at 373 K, then calcined in flowing air at 773 K with a ramp of 2 K/min and a final hold of 6 h. The catalysts prepared in this way are shown in Table 2.1

2.2 Incipient Wetness Impregnation

The precursor salts were either $Mn(NO_3)_2$ (Baker, 50.8 wt% in water), $(NH_4)_2Ce(NO_3)_6$ (Aldrich, 99.9%; FW = 548.25) or $La(NO_3)_3$*6 H_2O (Alfa Aesar, 99.9%; FW = 433.1) were dissolved in deionised water such that the volume of solution in mL was twice the weight of the support oxide in grams. For those supported on Al_2O_3 (Engelhard Al-3945E, 1/12") the wt% of alumina in the final oxide mixture was calculated at 80%. The solution was added either dropwise (small batches) or using an orbital shaker (large batches) to the support; the

impregnated oxide was dried at 423 K and then calcined in flowing air at 673 K with a 2 K/min ramp and a final hold of 2 h. The catalysts prepared in this way are shown in Table 2.1.

Table 2. 1 Sorbent compositions

Catalyst	**Composition(molar)**	**Method of preparation**
REOM_4	Ce/La = 0.9	SG
REOM_14	Ce/La = 3	SG
REOM4_Mn	M/(Ce+La) = 0.1	IWI
REOM4_Mn2	M/(Ce+La) =0.3	IWI
SRE-1	La/Zr = 0.88	IWI
SRE-2	Ce/La/Al = 3/1/53	IWI, 20 wt% Ce/LaO_x on Al_2O_3
SRE-3	Ce/La/Al = 0.9 /1/25	IWI, 20 wt% Ce/LaO_x on Al_2O_3
SRE-5	Tb/Ce/La/Al = 0.2/0.9/1/28	IWI, 20wt% Tb/Ce/LaO_x on Al_2O_3

2.3 Characterization of Oxide Sorbents/Catalysts

The BET surface areas of the oxides were measured by N_2 adsorption - desoprtion using a Quantachrome AS-1 BET apparatus. The oxides were first degassed by heating at 573 K for 1 hour under vacuum. The surface areas were computed from the adsorption branch of the isotherm by a 3-point BET algorithm.

XRD spectra of the powdered samples at high angles were obtained using a Rigaku miniflex 2005C103 X-Ray diffractometer (XRD) using Cu-Kα radiation. Samples were scanned from 5-60^o at 1^o/min with a 0.05^o step size. Low-angle XRD spectra were obtained on some samples using the powder XRD beamline at the LSU Center for Advanced Microsructures and Devices using Cu-Kα radiation. The samples were scanned from 0.5-10^o with a step size of 0.04^o, 6 s integration time. The spectra in both analyses were background subtracted and pattern

smoothed using MDI Jade software. A peak search algorithm was used to find the exact locations of the peaks.

2.4 Tar Cracking Reactions

Microreactor tests for tar (here, naphthalene) cracking were performed using a simulated gasifier effluent of 30.5 mol% CO_2, 22.2% H_2, 38.9% N_2, 8.0% H_2O, 0.022% H_2S, and 0.35% $C_{10}H_8$. To obtain such a low H_2S concentration a 0.4% H_2S/N_2 mixture was fed from a lecture bottle. Initially a 2% H_2S/N_2 mixture was prepared in a lecture bottle from H_2S (Matheson 99.9%) and N_2 (Airgas, UHP) cylinders. Then the 0.4% H_2S/N_2 mixture was prepared by mixing appropriate amounts of the 2% H_2S/N_2 and N_2 cylinders. A 40% H_2 / 60% N_2 mixture (Airgas, grade5) cylinder was used to add H_2, and a liquified CO_2 cylinder (Airgas, industrial grade) was used to add CO_2. The flow rates of the gases were adjusted to the required flow rates using manual flow controllers. The gas mixture was then passed through a water saturator maintained at 315 K, and then a naphthalene saturator maintained at 338 K. The naphthalene saturator was a ¼" stainless steel tube with glass wool on both ends. The naphthalene and water saturators were heated using heating tape, and the temperature was controlled using a variable transformer. Two K-type thermocouples were used to measure the temperatures of the saturators. The total gas flow rate was ~110 mL/min at STP. The reacting gas was then passed through the sorbent/catalyst maintained at 903 K. All the catalysts used for the tar cracking reactions had already been used in multiple cycles (regeneration-adsorption- desorption- regeneration) of desulfurization using essentially the same feed, minus the naphthalene.

The catalyst/sorbent itself (0.6-1.0 g with 0.001 g precision) was contained in a ¼" stainless steel U-tube filled with quartz wool on both ends. The U-tube was heated using a sand-filled furnace, controlled using a Eurotherm 818-p PID controller. A K-type thermocouple

measured the temperature of the sand bath. Prior to reaction the oxides were heated to 903 K in air (Industrial grade) flowing at 60 mL/min for 40 min and then the flow switched to He by a Valco 8-port valve operated by Red Lion Libra Timer. The He flow was turned off after 5 min and the reacting gas flow was started. The transfer lines were all maintained at 403 K to prevent condensation of naphthalene and water vapor. The gas was sampled using a 6-port Valco valve operated by the same timer. The gas was exhausted to a fume hood. A schematic of the system is shown in Figure 2.1.

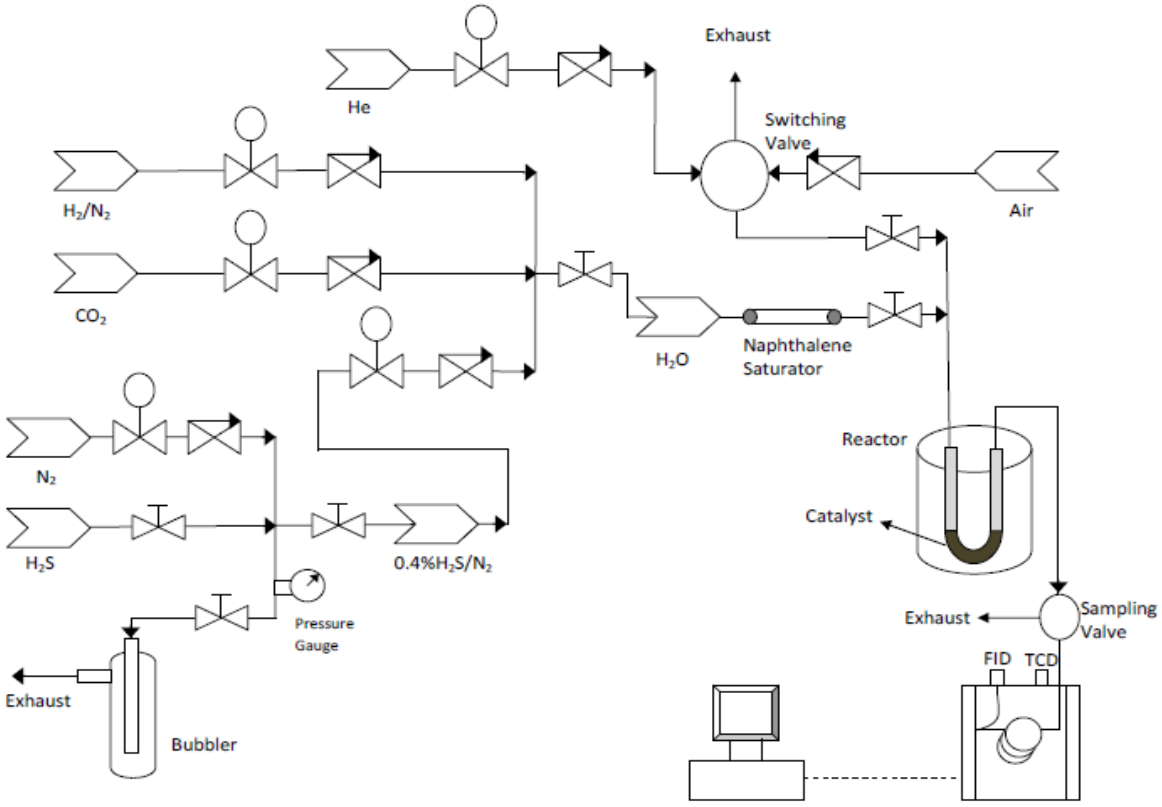

Figure 2. 1 Schematic of reactor system for tar cracking reactions

The gas from the sampling valve was analyzed in a HP 5800 Series-II GC. Samples were taken every 2 minutes, until the naphthalene concentration in the exiting gas was equal to that of the inlet gas. Further details on the GC analysis are given in Appendix A.

2.5 Sulfidation Tests

Sulfidation (adsorption) tests were performed at 903 K using a gas composition of 23.4 mol% H_2, 41.4% N_2, 3.1%H_2O, 32.0% CO_2, and 0.1% H_2S and GHSV of 15500h^{-1}. The gas mixture was prepared in the same way as described in the tar cracking reaction tests. For adding H_2S, a 2% H_2S/N_2 lecture bottle cylinder was used. The total flow rate of the gas was 100 mL/min at STP. The gas mixture from the cylinders was passed through the water saturator maintained at 298 K, then to the ½" stainless steel U-tube containing about 0.6-1.0g (with 10^{-8} precision) of oxide with quartz wool on both ends. The U- tube was controlled as in the tar cracking reactions. The exit gas was passed to a 10-port Valco sampling valve and analyzed using a sulphur-specific pulsed flame photometric detector (PFPD) attached to a Varian 3800 GC. Further details on the analysis are given in Appendix A. The sampling valve was maintained 373 K, and samples were taken until the sulfur concentration in the inlet gas was equal to that in the exit gas for at least 5 min. The exit gas from the sampling valve was exhausted to a fume hood. Prior to the tests, the catalysts were pretreated in the same way as in the tar cracking tests.

2.6 Temperature Programmed Desorption and Regeneration

After saturation of the sorbent, the feed flow was switched to He flowing at 60 mL/min. The temperature of the U-tube was raised from 703 to 1103 K at 10 K/min. The gas was sampled every 15 s. The sorbent was held at 1103 K until no sulfur was detected in the exiting gas, and it was then cooled to room temperature in He. All oxides used for either desulfurization or tar cracking experiments were regenerated in air flowing at 60 mL/min, 903K, for 40 min.

CHAPTER 3

RESULTS AND DISCUSSION

3.1 Characterization of Materials

Surface areas were measured for both fresh sorbents and for sorbents after use in multiple cycles of sulfidation/regeneration. These are shown in Table 3.1.

Table 3. 1 Surface area of sorbents before and after used in multiple cycles of sulfidation

Sorbent	**Composition**	**Surface area after calcination (m^2/g)**	**Surface area after multiple sulfidation/ TPD tests (m^2/g)**
REOM_14	Ce/La=3	242	98
REOM_4	Ce/La=0.9	110	40
SRE-1	La/Zr=0.8	65	43
SRE-2	Ce/La/Al=3/1/53	160	NA
SRE-3	Ce/La/Al=0.9/1/25	160	150
SRE-4	Gd/Ce/La/Al=0.2/0.9/1/28	160	120
SRE-5	Tb/Ce/La/Al=0.2/0.9/1/28	170	99
REOM4_Mn2	M/Ce+La=0.3	62	5

The average pore diameter calculated for REOM_14 using the desorption curve and the Barrett-Joyner-Halinda algorithm (BJH) is 3.83 nm and the pore volume is 0.23 cc/g (Kalakota 2008). The surface area of the unsupported REOs (REOM_4, REOM_14, REOM4_Mn2) decreased significantly during the sulfidation runs. This is due to the sintering of the REO nanoparticles or crystallites taking place at the high operating temperatures and high water

partial pressures used in the sulfidation runs. REOM_14 (Ce/La=3) retained more surface area than REOM_4 (Ce/La=0.9) indicating that sorbents containing high Ce/La are more resistant to sintering during the sulfidation runs. The REOs supported on Al_2O_3 and ZrO_2 (SRE-1, SRE-3, SRE-4, SRE-5) showed less reduction in surface area, since both supports increase the thermal stability of REOs (Yi et al., 2005; Trovarelli et al., 1997). Addition of third REO did not improve the surface area retention of the sorbents as was shown by SRE-4 and SRE-5. Reom4_Mn2 showed a very high percentage decrease in surface area, so possibly the surface Mn aids the sintering process.

The presence of crystalline phases and the average particle sizes of the crystallites were determined using XRD. The average particle size was determined using the Scherrer equation.

$$\beta = K \lambda / L_w \cos(\theta)$$

Where

K= 0.94

λ= wavelength of CuK_α radiation

L_w= the full width of the peak at half maximum (FWHM)

θ = the Bragg angle

The distance between atomic layers in a crystal (d) is calculated using Bragg's law:

$$n \lambda = 2 d \sin\theta$$

Where

n is an integer

λ= wavelength of CuK_α radiation

θ = the Bragg angle

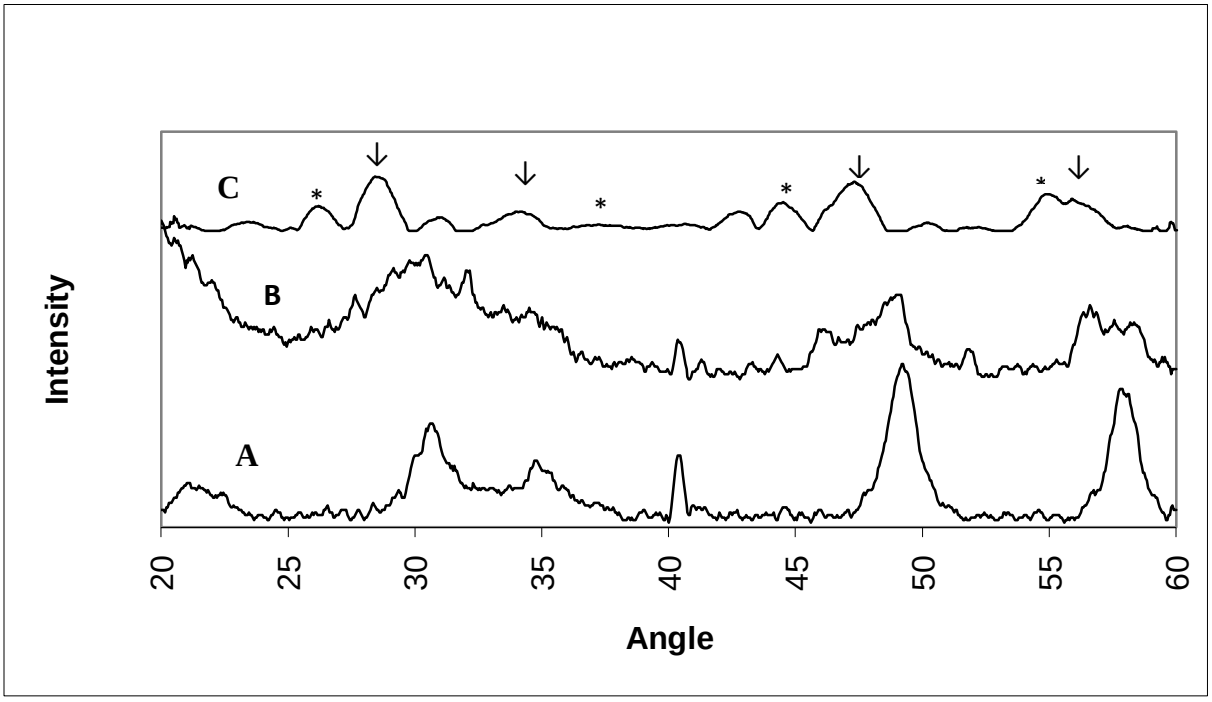

Figure 3. 1 XRD analysis of Mn-containing sorbents (as calcined): (A) REOM_4 (B) REOM4_Mn (C) REOM4_Mn2

***indicates β-MnO_2 peaks**

↓indicates CeO_2 peaks

REOM_4 (Ce/La=0.9) was scanned from 20-60º with 0.05º step. The peaks at 30.7º, 34.9º, 49.3º, 58.1º correspond to (1 1 1), (2 0 0), (2 2 0) and (3 1 1) reflections of cubic fluorite CeO_2 phase (JCPDS 43-1002). The peak at 40.5º which is visible in all Ce/LaOx could not be identified. The particle size calculated using (1 1 1) reflection of CeO_2 phase is 8.7nm. The sorbents containing La are shifted towards higher 2θ values by ~2º compared to pure CeO_2 (Kalakota 2008). The shifts towards higher 2θ indicate formation of a ceria-lanthana solution (Bernal et al., 1998).

REOM4_Mn (M/(Ce+La)=0.1) was also scanned from 20-60º degrees with 0.05º step. The peaks are broad denoting the lack of a significant "long-range" crystalline order. The peaks at 30.5º, 34.7º, 49.2º and 57.9º correspond to (1 1 1), (2 0 0), (2 2 0) and (3 1 1) reflections of the cubic fluorite CeO_2 phase. Like REOM_4, the peaks are shifted towards higher 2θ values by 2º. The presence of a separate LaO_x and MnO_x like phase was not detected. This indicates that both La and Mn have been in large part dispersed into the ceria phase. The particle size calculated using the (1 1 1) reflection of the CeO_2 phase is 2.5nm.

REOM4_Mn2 (M/(Ce+La)= 0.3) was scanned from 20-60º with 0.04º step and 4 s integration time. The phases identified in REOM4_Mn2 are the cubic fluorite CeO_2 and β-MnO_2. The peaks at 28.6º, 34.3º, 47.3º and 56º correspond to (1 1 1), (2 0 0), (2 2 0) and (3 1 1) reflections of the CeO2 phase respectively (JCPDS 43-1002). The peaks at 26.3º, 37.3º, 44.6º and 55º correspond to the (1 1 0), (1 0 1), (1 1 1) and (2 1 1) reflections of the β-MnO_2 phase (JCPDS 24-0735). The peaks shifted towards lower 2θ values by 0.5º. The particle size calculated using the (1 1 1) reflection of CeO_2 phase is 8.93 nm. The particle size calculated using (1 1 0) reflection of the MnO_2 phase is 10.6 nm. The large particle sizes are consistent with the low surface area of the "as calcined" material in Table 3.1.

The alumina-supported REOs, SRE-2 (Ce/La/Al= 3/1/53), SRE-3 (Ce/La/Al= 0.9/1/25) and SRE-5 (Tb/Ce/La/Al= 0.2/0.9/1/28), were scanned from 20-60º with a 0.05º step. Most of the peaks are broad denoting the lack of a significant "long-range" crystalline order. The phase identified in SRE-2 is CeO_2. The (1 1 1), (2 0 0), (2 2 0) and (3 1 1) reflections of CeO_2 phase were observed at 30.45º, 34.7º, 49.05º and 58.05º. The peaks were shifted towards higher 2θ values by 2º. This is consistent with the formation of a ceria- lanthana solid solution (Bernal et al., 1998). The particle size of SRE-2 calculated using the (1 1 1) reflection of the CeO_2 phase is 6.6 nm. The broad peak between 46º and 51º observed in SRE-2,3,5 is likely an overlap of the (2

2 0) reflection of CeO_2 phase and a reflection characteristic of the γ- Al_2O_3 phase (JCPDS 29-63). SRE-3 and SRE-5 showed mostly low intensity and broad peaks of the CeO_2 phase indicating low crystallinity. The high intensity peak at 40.45º in SRE-3 could not be identified.

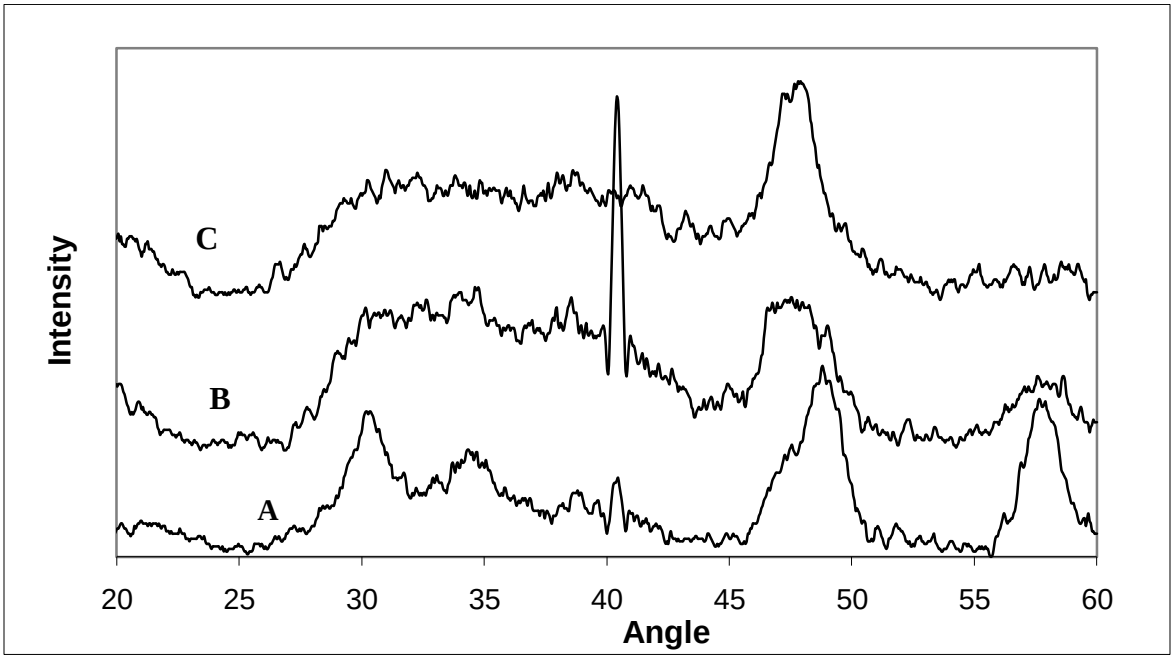

Figure 3. 2 XRD analysis of supported Ce/La sorbents: (A) SRE-2 (B) SRE-3 (C) SRE-5

SRE-1 was also scanned from 20-60º with a 0.05º step. It contained a mixture of the monoclinic, tetragonal and cubic crystalline structures of zirconia (Juutilainen et al., 2006). The (1 1 1) reflection of t-ZrO_2 was observed at 2θ= 32.35º. The reported position for the (1 1 1) reflection of t-ZrO_2 is at 2θ= 30.306º (Barshilia et al., 2008). The peaks at 30.45º, 33.55º and 57.43º correspond to (1 1 1), (0 0 2) and (0 1 3) reflections of m-ZrO_2 (JCPDS 13-307). The peaks at 36.9º and 52.3º correspond to peaks of the cubic ZrO_2 phase (JCPDS 27-997). No LaO_x diffraction peaks were observed. This indicates that lanthana formed a solid solution with zirconia such that the only XRD detectable phase is ZrO_2. The particle size calculated using the (1 1 1) reflection of t-ZrO_2 is 19.1 nm.

The supposedly mesoporous REOs REOM_4 (Ce/La= 0.9) and REOM_14 (Ce/La= 3) were scanned from 0.5-10º with a 0.02° step in order to estimate the dominant pore size from the largest d-spacing. NIST Mica 675 standard was used to verify the correct 2θ offset. The large decay at 0.5-0.85º is characteristic of the instrument and not associated with the sample. For REOM_4, the d-spacing calculated using Bragg's law for the peak at 2θ = 0.92º is 9.6 nm. For REOM_14, the d-spacing calculated for the peak at 2θ = 1.24º is 7.1 nm. The average pore diameter for REOM_14 is 3.83 nm. Therefore the calculated total wall thickness for REOM_14 is 3.3 nm. The total wall thicknesses of CeO_2 mesopores from the literature are reported to be between 3 and 5 nm (Chane-Ching et al., 2005).

3.2 Sulfur Adsorption and TPD Tests

The sulfur adsorption capacity of the sorbents was determined using a synthetic gasifier effluent reaction mixture containing 23.4 mol% H_2, 41.4% N_2, 3.1% H_2O, 32.0% CO_2, and 0.1% H_2S. Adsorption tests were done at 903K and atmospheric pressure. TPD tests were done using He as carrier gas from 903K to 1103K. The former tests gave the maximum sulfur adsorption capabilities of the sorbents while the latter tests gave the amount of sulfur that can be easily desorbed. Since both the stainless steel U- tube and the quartz wool adsorb sulfur, blank tests were done first in order to find the exact amount of sulfur adsorbed by these. The amount of H_2S adsorbed only by the sorbent was then determined by subtracting the amount obtained from the blank tests at the respective times. In order to eliminate fluctuations in the runs, multiple blank tests were performed and the average of 6 runs was used. Blank runs were performed by passing the reaction mixture through the U-tube for 5 minutes and then switching to He and ramping the temperature from 903K to 1103K.

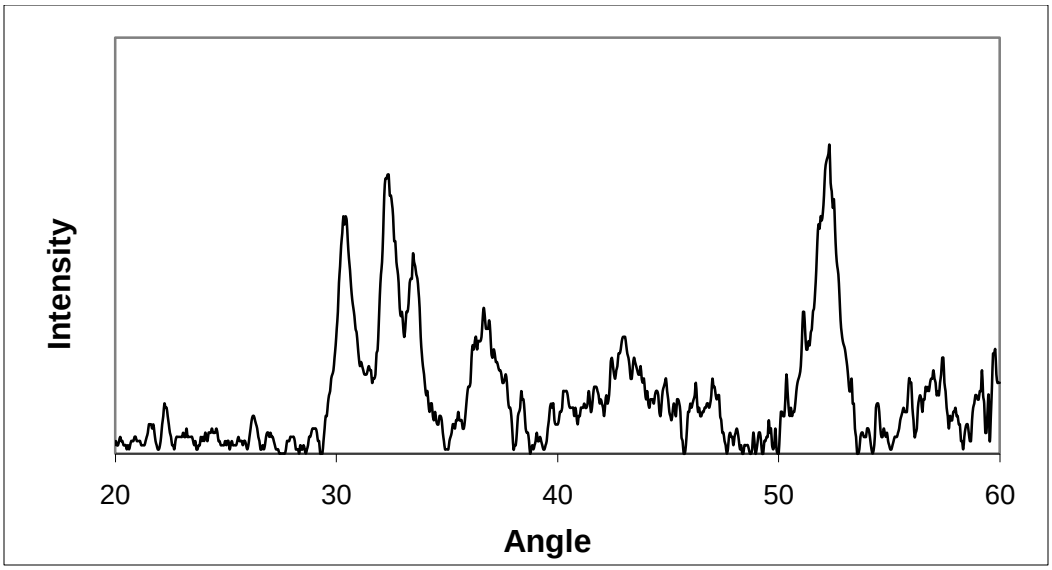

Figure 3. 3 XRD analysis of SRE-1

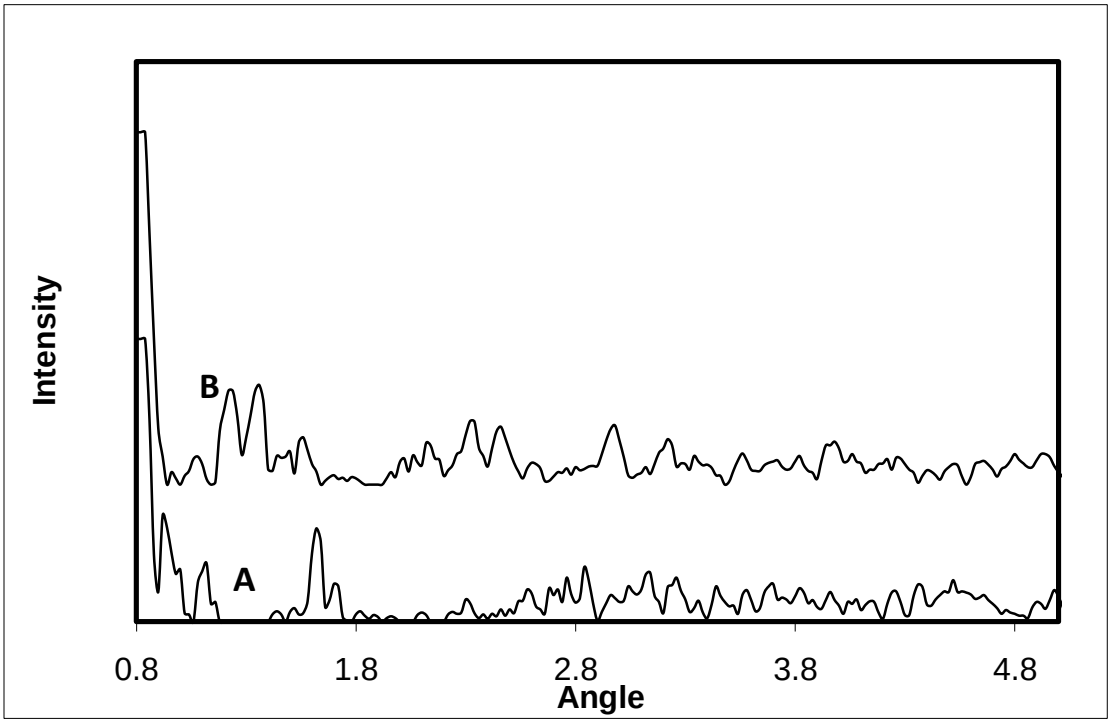

Figure 3. 4 XRD analysis of sorbents. (A) REOM_4 (B) REOM_14

$$A_B = (A_1+A_2+A_3+A_4+A_5+A_6) / 6$$

Where A_1, A_2, A_3, A_4, A_5, A_6 are the areas (proportional to the amount of sulphur) given by the GC detector at time t during the six blank tests.

For the non-blank runs:

$$A_S = A_A - A_B$$

Where,

A_A is the area given by the GC at time t of the actual run using sorbent

A_S is the corrected area for the absolute amount of sulfur.

The corrected areas were then smoothed using a three point average over 0.5 min:

$$A_T = (A_{s-0.25} + 2As + A_{s+0.25}) / 4$$

Where,

$A_{s-0.25}$ is the area given by GC at time t-0.25

A_s is the area given by GC at time t

$A_{s+0.25}$ is the area given by GC at time t+0.25

A_T is the corrected area at time t

The micromoles of sulfur at time t (μ_t) were then found from:

$$\mu_t = A_T \ CF$$

Where CF (µmole/Area) is the calibration factor - see Appendix A for how this was obtained.

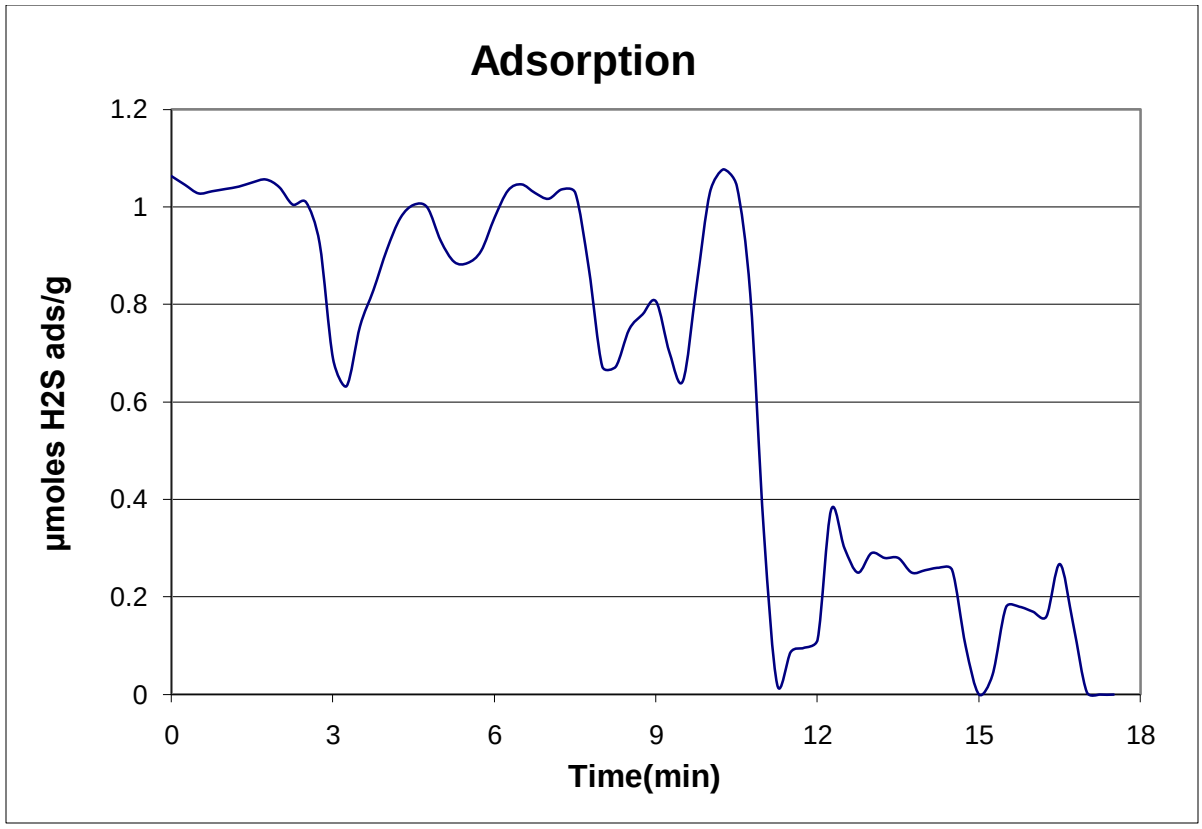

Figure 3. 5 Amount of H2S adsorbed vs time for REOM4_Mn (4th run).

The micromoles of sulfur/g of sorbent exiting the reactor from t-1 to t was calculated as:

$$\mu_t = [(\mu_{t-1}+\mu_t) / 2] \ (F_G / V_S) \ (t_S / W_S) \ (T_S / T_0)$$

Where

F_G is the total gas flow rate at STP

V_S is the volume of sampling loop

t_S is the time increment between samples

W_S is the weight of sorbent

T_S is the temperature of sampling loop, 373K

T_0 is 273 K

μ_T is the micromoles of sulfur/g of sorbent exiting the reactor at time t

The total micromoles of sulfur desorbing from the sorbent is found from:

$$\mu_{total} = \sum_{t=0}^{t_f} \mu_t$$

where t_f is the time of the desorption of removable sulfur

Total micromoles of sulfur entering the reactor during a run (μ_e) is found as:

$$\mu_E = (\text{Flow rate of } H_2S)\ (1/22400)\ (T_0/T_A)\ t$$

where

t is the time to attain saturation of the sorbent

T_A is ambient temperature, 298K

The total micromoles of sulfur adsorbed is then:

$$\mu A = \mu_E - \mu_{total}$$

Several sorbents were tested in multiple cycles of adsorption- desorption- regeneration. The sulphur adsorption capacities of REOM_4, REOM_14, SRE-5, SRE-2, SRE-3 and REOM4_Mn are shown in Figures 3.6, 3.7 and 3.8. For each sorbent, the cycle was repeated until the adsorption capacity showed increases of less than 30%. The maximum capacities for SRE-1 and REOM4_Mn2 were previously measured by Kalakota (2008). These maximum sulfur capacities were compared to a commercial BASF Selexsorb CDX 7 X 14 mesh sorbent

composed of Al_2O_3/Zeolite with 15 – 40% Zeolite of unspecified phase. The adsorption and desorption capacities of this sorbent (Kalakota 2008) are shown in Figure 3.6. The initial capacity of this sorbent is very high but the capacity decreased sharply in the following run; it is not stable at these conditions.

The sulfur capacities of the supported rare earth oxides were in general found to be greater than that of the unsupported REOs, especially if compared on a basis of per weight of REO - the active weight of the SREs is only 20% of the total sorbent weight. This is because supporting monolayers or nanoparticles of REOs on either Al_2O_3 and ZrO_2 supports improves the thermal and steam stability of the REOs (Yi et al., 2005; Trovarelli et al., 1997). However, the Al_2O_3 on which SRE2-5 were supported has very low sulfur capacity.

Among the sorbents tested, REOM4_Mn (M/(Ce+La)= 0.1) gave the highest and REOM_14(Ce/La= 3) gave the lowest sulfur capacities. Impregnation of REOs with Mn greatly improved the sulfur removal capacity of the sorbents. The capacity of this sorbent is in the range 90-180 μmoles of H_2S /g of sorbent; sulfur capacities of REOs impregnated with transition metals are in the order Mn > Fe >> Cu (Kalakota 2008). The capacities of REOs tested here are in the range 20-50 μmoles of H_2S/g of sorbent. The observed capacities of Ce and La mixed sorbents are in the range of 25 to 250 μmoles of H_2S adsorbed/g of sorbent for a gas composition of 0.1% H_2S, 50% H_2, 10% H_2O, balance He at 923 K (Flytzani-Stephanopoulos et al., 2006; Wang and Flytzani-Stephanopoulos, 2005). From this it can be concluded that the unsupported Ce/La REOs are not very effective in removing H_2S from a more realistic gasifier effluent containing CO_2. At monolayer loading the adsorption capacity of 25wt% Mn/Al_2O_3 using the same feed used in this work and tested at 873K is 29μmole of H_2S/g of sorbent (Kalakota 2008). For Ce/Mn oxide sorbents with a Ce/Mn ratio varying from 0.66 to 3, for a gas

composition of 1% H_2S and 10% H_2, balance He the observed capacities for multiple runs are in the range of 610 to 1150 µmole S/g of sorbent at 873 K (Yasyerli, 2008). The capacities of the Mn sorbents tested in this work were lower probably because the feed gas also consists of CO_2 and H_2O, both of which compete for active sites on the sorbent and decrease capacity.

Among the supported rare earth oxides (SREs), SRE-5 (Tb/Ce/La/Al= 0.2/0.9/1/28) containing a small amount of Tb_2O_3 gave the highest sulfur removal capacity. This indicates that addition of a third REO improves the sulfur removal capacity. This may be due to the increased oxygen vacancies provided by the third REO (Bernal et al., 2002; Huang et al., 2005). For SRE-5, the sorbent capacity increased in the first three runs and then stabilised. This may be due to the formation of solid solution of the three REOs present in this sorbent. The capacity of this sorbent is slightly greater than a similarly prepared Gd/Ce/La/Al_2O_3 sorbent (Kalakota 2008).

From the TPDs, the amounts desorbed in inert gas were calculated and these are shown in red in Figures 3.6 - 3.8. The amount of sulfur desorbed was approximately 50% of that adsorbed. From the TPDs it is clear that inert gas itself is not sufficient to remove all the adsorbed sulphur, but that much of it is weakly bound. This is in agreement with the literature for REOs (Wang and Flytzani Stephanopolous, 2005).

3.3 Tar Cracking / Removal

Simultaneous tar cracking and desulfurization experiments were performed using a gas composition similar to that of the previous experiments: 30.5 mol% CO_2, 22.2% H_2, 38.9% N_2, 8.0% H_2O, 0.022% H_2S, and 0.35% $C_{10}H_8$. To measure the tar cracking capability of the non-sulfided catalysts, experiments were run using essentially the same molar composition, but with N_2 replacing H_2S. All of the sorbents used in the tar cracking tests had already been used in

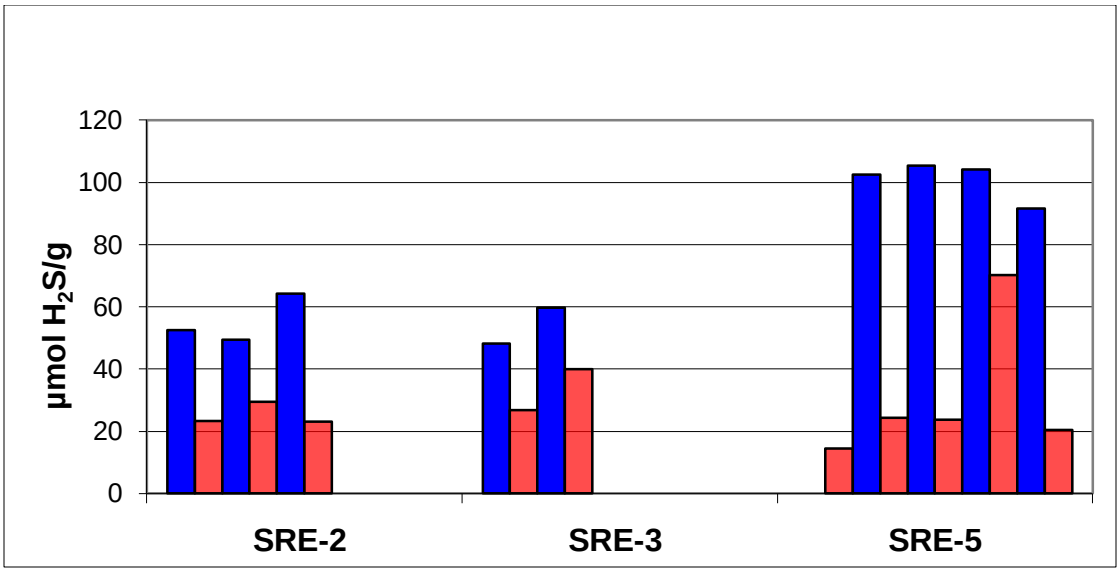

Figure 3. 6 Adsorption (dark) and desorption (light) capacities of SRE-2, SRE-3 and SRE-5 sorbents.

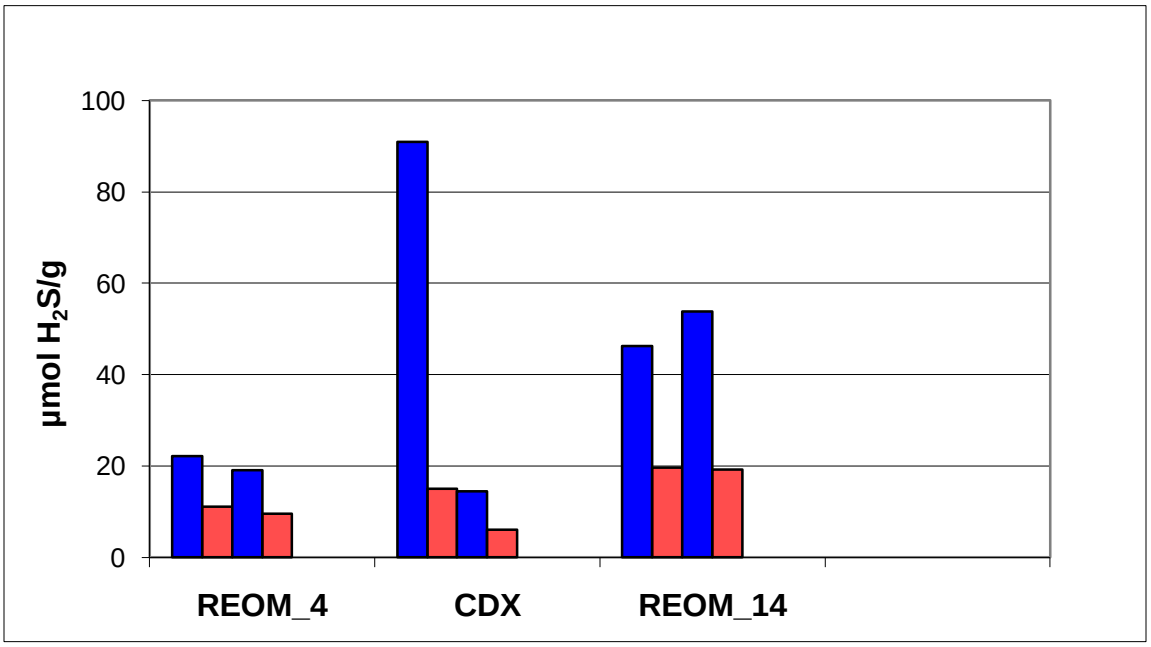

Figure 3. 7 Adsorption (dark) and desorption (light) capacities of Reom_4, CDX, Reom_14 sorbents.

.

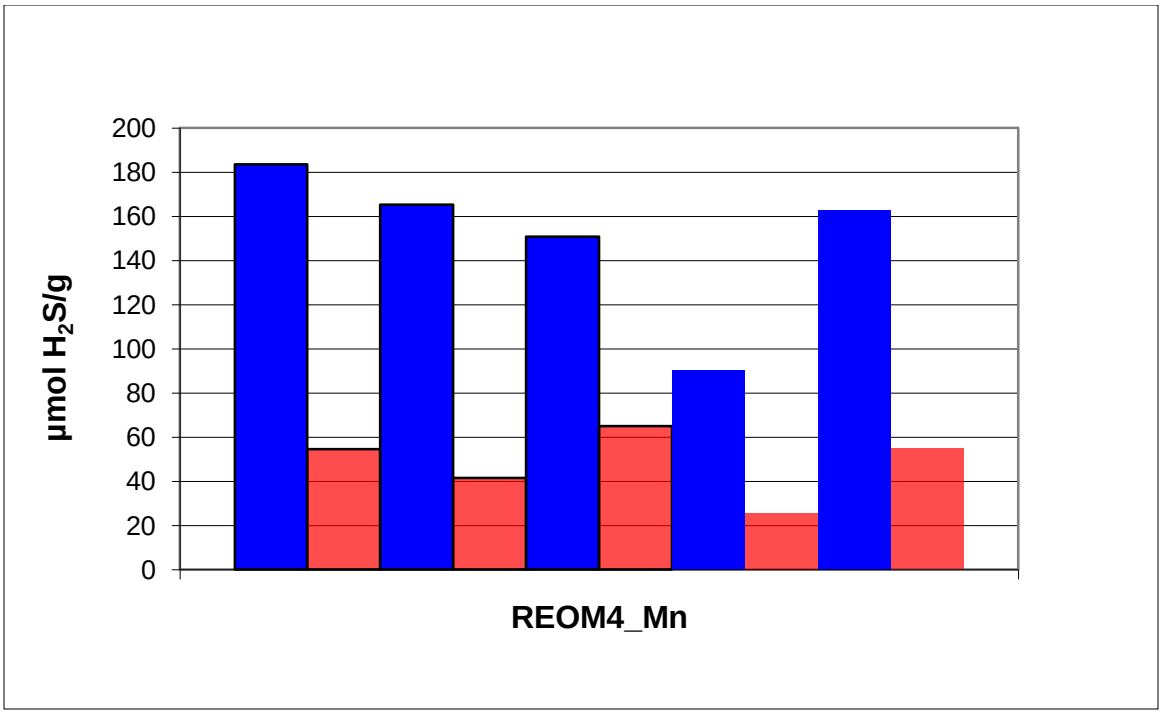

Figure 3. 8 Adsorption (dark) and desorption (light) capacities of REOM4_Mn.

multiple sulfidation cycles, except where noted in Tables 3.1-3.2 below. All of the tar cracking experiments were done at 903 K and atmospheric pressure.

The % of naphthalene adsorbed and reacted at time t was calculated as:

$$R_t = 100 - (A_t / A_A)\ (100)$$

Where

A_t is area measured by GC at time t

A_A is the average of the areas of the naphthalene feed

The moles of naphthalene removed (reacted and/or adsorbed) at time increment n (M_n) was calculated as:

$$M_n = (R_t/100)\ (CF\ A_A / M_B)\ y_f\ (F_G / 22400)\ (273/298)$$

Where,

CF is the calibration factor, µmoles naphthalene/area.

M_B is the maximum number of moles of naphthalene in the sampling loop (for the feed)

y_f is the mole fraction of naphthalene in the feed

F_G is the flow rate of reaction gas mixture

The amount of naphthalene reacted over the time period Δt was then calculated by the trapezoidal rule.

$$\mu_t = [\Delta t] \quad [(M_n + M_{n-1}) / 2] \, 10^{-6}$$

The total micromoles (µtotal) of naphthalene reacted over 30 minutes t_f was calculated as:

$$\mu\text{total} = \sum_{t=0}^{t_f} \mu_t$$

Table 3. 2 Tar removal of naphthalene and sulfur capacities of sorbents used for multiple sulfidation cycles

Sorbent	Composition	µmoles of tar removed in 30 min with feed containing H_2S	µmoles removed in 30 min for H_2S-free feed	µmoles of H_2S adsorbed in 30 min (averaged capacities)
SRE-1	La/Zr=0.8	22	30	120
SRE-5	Tb/Ce/La/Al= 0.2/0.9/1/28	20	42	100
Reom_14	Ce/La=0.3	40	67	51
Reom4_Mn	M/(Ce+La)= 0.1	44	45	160
Reom4_Mn2	M/(Ce+La)= 0.3	57	100	150

Table 3. 3 Tar removal of naphthalene and sulfur capacities of fresh sorbents

Sorbent	µmoles of tar removed in 30 min with feed containing H_2S	µmoles of H_2S adsorbed in 30 min
SRE1	32	120
Reom4_Mn2	24	150

The sulfur capacities and percentages of naphthalene removed are compared in Fig. 3.9. The numbers for µmol naphthalene removed refer to sorbents already used in multiple sulfidation/TPD cycles and for feeds containing H_2S, as in Table 3.2. The sulfur capacities shown are the average capacities over multiple cycles.

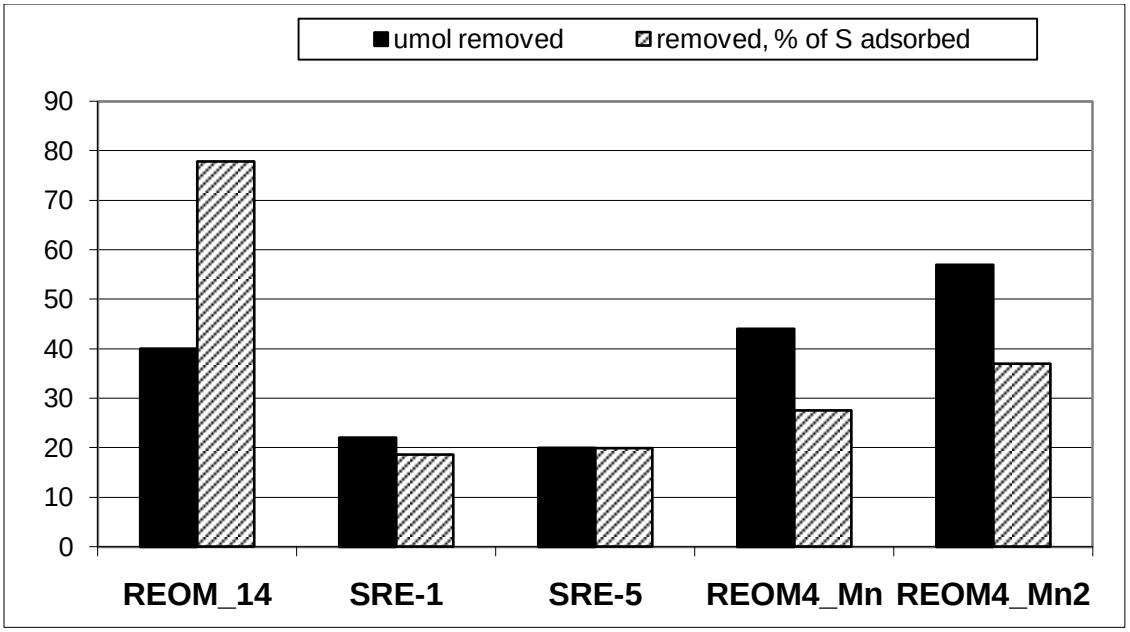

Figure 3. 9 Comparision of naphthalene removal and sulphur capacities of sorbents

Among the sorbents tested, the REOs impregnated with Mn have the highest capacity for the simultaneous removal of tars and desulfurization. The capacity for tar removal and desulfurization increased with an increase in the Mn/REO molar ratio from 0.1 to 0.3. The

supported REOs, which showed higher sulphur removal capacities compared to unsupported REOs, showed a lower capacity for tar removal. Among the supported REOs, the one supported on ZrO_2 showed slightly higher tar removal and desulfurization capability compared to those supported on Al_2O_3. The advantage is even greater if compared on a surface area basis. This may be because lanthana is completely miscible in zirconia and formed a homogeneous solid solution as suggested by XRD. These results suggest that the intimate contact between zirconia and lanthana is favourable for the naphthalene conversion. When the sorbents were tested only for tar removal, without H_2S in the reaction mixture, all sorbents showed higher tar removal capability as expected. The total tar removed increased significantly, in some cases almost doubling, for all the sorbents except for Reom4_Mn. Among the fresh sorbents tested, a supported REO such as SRE1 showed slightly higher tar removal than one already used in multiple sulfidation cycles, as might be expected. However, fresh Reom4_Mn2 actually removed less naphthalene when compared to Reom4_Mn2 used in multiple sulfidation cycles. This may be because there is some miscibility or spreading of Mn taking place that enhances both the desulfurization capacity and the tar removal capability. Comparing all the sorbents, it can be concluded that Reom4_Mn2 has the highest capability for simultaneous tar removal and desulfurization of gasifier effluents. This may be because both MnO_2 and lanthana formed a solid solution with ceria, as suggested by the XRD results of REOM_4 and REOM4_Mn. But a separate MnO_2 phase was observed in REOM4_Mn2 (more active) which was absent in REOM4_Mn (less active). Mn ions are initially incorporated into CeO_2 defect sites, possibly catalyzing the sintering of ceria which took place. Above a critical concentration, Mn then occupies the lattice sites at outer layers of the crystallites (Murugan et al., 2005). Both the ceria-lanthana solid solution and the other unknown form of Mn must be effective in removing tar and

H_2S, as REOM4_Mn2 showed better tar and H_2S removal capability compared to REOM4_Mn, while simple supported (on Al_2O_3) MnO_2 is almost inactive.

GC-MS analyses of the gas phase were performed on REOM4_Mn with the same gas feed but with N_2 substituting for H_2S. Samples were collected into gas bags every 10 minutes and injected into a GC-MS. The easily identifiable components in the samples were N_2, CO_2 and naphthalene. Since all the light gases (N_2, CO_2 etc.) eluted together on the GC column, it was not possible to distinguish CO, H_2, ethylene, or propane in the presence of so much N_2 and CO_2. There were traces of CH_4 and C_2H_6 in all samples, so C_2H_4 was probably there in trace amounts also. There was no propylene, so propane was probably not present (within detection limits, which were about 10 ppm). Traces of benzene were also found in all samples.

The initial tar conversion was 10-45% for all the sorbents tested with H_2S in the feed but the conversion decreased with time. The initial tar conversion was 18-50% for sorbents tested without H_2S in the feed. All the catalysts tested deactivated in 30 minutes or less. In the case of feeds without H_2S, this may be due to the formation of coke on the surface of the sorbents blocking the active sites. Complete naphthalene conversion was achieved using a MgO - supported nickel catalyst tested at 1073K using a feed containing 49.8% N_2, 12% CO, 10% H2, 11% CO_2, 5% CH_4 and 12% H_2O, 0.3% naphthalene and 100 ppmv H_2S, with a GHSV of 2080 h^{-1}. The catalyst was stable for 100 h (Nacken et al., 2007). The high reforming activity and stability of this catalyst compared to the sorbents tested in this work may be due to the high temperature and low GHSV used, and the small amount of sulfur present.

The tar conversion using Ni/MgO catalysts at 873 K and a feed composition of $C_{10}H_8/C_6H_6/H_2O/N_2/Ar$ = 0.3/2.7/19.2/10.0/67.8 mol% with a GHSV of 19,200 h^{-1} was ~40% for 2 h and decreased to 10% after 10 h reaction (Furusawa et al., 2009). The higher activity and

stability of these catalysts compared to sorbents tested in this work may be due to the absence of both H_2S and CO_2 in the feed. In the literature most of the tar reforming experiments were done without H_2S in the feed. Adding H_2S to the feed should reduce the tar reforming capability of the sorbents since H_2S also competes for active sites and is adsorbed irreversibly. However, there is no doubt that adding Ni to the present materials would greatly increase the rates of tar cracking or reforming. For example, 90% tar conversion at 1073-1123K was reported for a Ni-WO_3/MgO-CaO catalyst with a feed consisting of 20% H_2, 5% CO, 5% CO_2, 3.5% tar (naphthalene / toluene), 0-500 ppm H_2S, 18% H_2O and balance N_2, with a GHSV of 14000 h^{-1}. This catalyst was stable for 100 h (Sato and Shinoda 2007) in the presence of 500 ppm of H_2S.

The sulfur adsorption capability of the sorbents tested in this work was found to be higher than that of the commercial sorbent CDX. The tar removal capacities of the sorbents tested were lower than some of the catalysts tested in literature. However, adding Ni to the present materials may greatly increase the rates of tar cracking or reforming.

CHAPTER 4

CONCLUSIONS

Ce/La oxides, Ce/La/M (M = transition metal) oxides and Ce/La/REO/Al_2O_3 (REO = a third rare earth oxide) sorbents were studied for the simultaneous desulfurization and tar reforming of synthetic biomass gasifier effluents. These sorbents were prepared by sol-gel and impregnation methods. Surface areas of the sorbents were determined by the BET method and the crystalline phases were determined using XRD. Multiple cycles of sulfidation and regeneration were carried out to evaluate the sulfur removal capacity and stability of the sorbents. Sulfidation tests were done using a simulated gas feed at 903 K. The alumina-supported sorbents retained most of their surface area even when exposed to high temperatures (1103 K) and hence are stable at the high operating temperatures of the gasifiers. Sulfur removal capacity of the pure Ce/La oxide sorbents was relatively low, but in agreement with the literature. Supporting Ce/La oxide on Al_2O_3 or La oxide on ZrO_2 improved the sulfur removal capacity of the sorbents compared to unsupported REOs, especially when compared on an active (REO) weight basis. Addition of a third rare earth oxide to SREs increased the sulfur removal capacity and the capacity retention of the sorbents. Among all sorbents tested, the Ce/La REOs impregnated with Mn showed the highest sulfur capacities. TPD tests were carried out from 903K to 1103K using He as carrier gas. It can be concluded from the adsorption and desorption capacities of the sorbents that inert gas itself is not sufficient to remove most of the adsorbed sulfur.

Sorbents with higher desulfurization capacities were tested for tar reforming using naphthalene as a simutaled tar. The sorbents showed 10-50% tar removal initially but the tar removal decreased as time progressed. All the catalysts deactivated over the same time scale.

Among all the sorbents tested, Reom4_Mn2 was found to be the best sorbent for simultaneous desulfurization and tar reforming of gasifier effluents.

4.1 Recommendations

- Regeneration of the sorbents should be carried out with other gas mixtures since regeneration using air is a highly exothermic process which may lead to thermal sintering.
- Characterization of the sorbents after sulfidation and after regeneration must be carried out in order to understand the changes in their surface structure.
- The sorbents must be tested for tar reforming in multiple cycles in order to understand the performance of regenerated catalyst.
- GC-MS tests should be conducted in order to find the products of tar cracking.

REFERENCES

Abu El-Rub, Z., Bramer, E. A., Brem, G., 2004 "Review of catalysts for tar elimination in biomass gasification processes", *Ind. Eng.Chem.Res* 43, p337-346.

Alonso, L., and Palacios, J. M., 2002 "Performance and recovering of a Zn-doped manganese oxide as a regenerable sorbent for hot coal gas desulfurization", *Energy & Fuels* 16, p1550-1556.

Arauzo, J., Radlein, D., Piskorz, J., and Scott, D. S., 1994 "A new catalyst for the catalytic gasification of biomass", *Energy & Fuels* 8, p1192-1196.

Arauzo, J., Radlein, D., Piskorz, J., and Scott, D. S., 1997 "Catalytic pyrogasification of biomass. Evaluation of modified nickel catalysts", *Industrial & Engineering Chemistry Research* 36, p67-75.

Asadullah, M., Ito, S., Kunimori, K., and Tomishige, K., 2002 "Role of catalyst and its fluidization in the catalytic gasification of biomass to syngas at low temperature", *Industrial & Engineering Chemistry Research* 41, p4567-4575.

Asadullah, M., Kunimori, K., and Tomishige, K., 2001 "Catalytic gasification of biomass to produce synthesis gas at low temperature", *Abstracts of Papers of the American Chemical Society* 222, 41-FUEL.

Asadullah, M., Miyazawa, T., Ito, S., Kunimori, K., and Tomishige, K., 2003 "Catalyst performance of Rh/CeO2/SiO2 in the pyrogasification of biomass", *Energy & Fuels* 17, p842-849.

Atakul, H., Wakker, J. P., Gerritsen, A. W., and Vandenberg, P. J., 1995 "Removal of H2S from fuel gases at high-temperatures using MnO/gamma-Al2O3", Fuel 74, p187-191.

Atakul, H., Wakker, J. P., Gerritsen, A. W., and vandenBerg, P. J., 1996 "Regeneration of MnO/gamma-Al2O3 used for high-temperature desulfurization of fuel gases", *Fuel* 75, p373-378.

Aznar, M. P., Caballero, M. A., Gil, J., Martin, J. A., and Corella, J., 1998 "Commercial steam reforming catalysts to improve biomass gasification with steam-oxygen mixtures. 2. Catalytic tar removal", *Industrial & Engineering Chemistry Research* 37, p2668-2680.

Bakker, W. J. W., Kapteijn, F., and Moulijn, J. A., 2003 "A high capacity manganese-based sorbent for regenerative high temperature desulfurization with direct sulfur production conceptual process application to coal gas cleaning", *Chemical Engineering Journal* 96, p223-235.

Bakker, W. J. W., Vriesendorp, M., Kapteijn, F., and Moulijn, J. A., 1996 "Sorbent development for continuous regenerative H2S removal in a rotating monolith reactor", p713-718.

Bampenrat, A., Meeyoo, V., Kitiyanan, B., Rangsunvigit, P., and Rirksomboon, T., 2008 "Catalytic oxidation of naphthalene over CeO2-ZrO2 mixed oxide catalysts", *Catalysis Communications* 9, p2349-2352.

Bangala, D. N., Abatzoglou, N., Martin, J. P., and Chornet, E., 1997 "Catalytic gas conditioning: Application to biomass and waste gasification", *Industrial & Engineering Chemistry Research* 36, p4184-4192.

Barshilia, C. H., Deepthi, B., Rajam, K. S., 2008 " Stabilization of tetragonal and cubic phases of ZrO2 in pulsed sputter deposited ZrO2/Al2O3 and ZrO2/Y2O3 nanolayered thin films", *Journal of Applied Physics* 104, p113532(1-12).

Benslimane, R., and Hepworth, M. T., 1994 "Desulfurization of hot coal-derived fuel gases with manganese-based regenerable sorbents .1. loading (sulfidation) tests", *Energy & Fuels* 8, p1175-1183.

Bernal, S., Blanco, G., Cauqui, M. A., Cifredo, G. A., Pintado, J. M., and Rodriguez-Izquierdo, J. M., 1998 "Influence of reduction treatment on the structural and redox behaviour of ceria, La/Ce and Y/Ce mixed oxides", *Catalysis Letters* 53, p51-57.

Bernal, S., Blanco, G., Cifredo, G. A., Delgado, J. J., Finol, D., Gatica, J. M., Rodriguez-Izquierdo, J. M., and Vidal, H., 2002 "Investigation by means of H-2 adsorption, diffraction, and electron microscopy techniques of a cerium/terbium mixed oxide supported on a lanthana-modified alumina", *Chemistry of Mat*erials 14, p844-850.

Bui, T., Loof, R., and Bhattacharya, S. C., 1994 "Multistage reactor for thermal gasification of wood", Energy 19, p397-404.

Caballero, M. A., Aznar, M. P., Gil, J., Martin, J. A., Frances, E., and Corella, J., 1997 "Commercial steam reforming catalysts to improve biomass gasification with steam-oxygen mixtures .1. Hot gas upgrading by the catalytic reactor", *Industrial & Engineering Chemistry Research* 36, p5227-5239.

Caballero, M. A., Corella, J., Aznar, M. P., and Gil, J., 2000 "Biomass gasification with air in fluidized bed. Hot gas cleanup with selected commercial and full-size nickel-based catalysts", *Industrial & Engineering Chemistry Research,* 39, p1143-1154.

Chane-Ching, Y,J., Cobo, F., , Aubert,D., Harvey,G, H., Airiau, M., and Corma, A., 2005 " A general method for the synthesis of nanostructured large-surface-area materials through the self-assembly of functionalized nanoparticles" *Chem. Eur. J,* 11, p979 – 987

Coll, R., Salvado, J., Farriol, X., and Montane, D., 2001 "Steam reforming model compounds of biomass gasification tars: conversion at different operating conditions and tendency towards coke formation", *Fuel Processing Technology* 74, p19-31.

Colon, G., Navio, J.A., Monaci, R. and Ferino, I., 1998 "CeO2 – La2O3 catalytic system Part I. Preparation and characterization of catalysts", PCCP, 200, 2, p4453-4459.

Corella, J., Aznar, M. P., Gil, J., and Caballero, M. A., 1999 "Biomass gasification in fluidized bed: Where to locate the dolomite to improve gasification?", *Energy & Fuels* 13, p1122-1127.

Costa-Nunes, O., Ferrizz, R. M., Gorte, R. J., and Vohs, J. M., 2005 "Structure and thermal stability of ceria films supported on YSZ(100) and alpha-Al2O3(0001)", *Surface Science* 592, p8-17.

Courson, C., Makaga, E., Petit, C., and Kiennemann, A., 2000 "Development of Ni catalysts for gas production from biomass gasification. Reactivity in steam- and dry-reforming", p427-437.

Dalai, A. K., Sasaoka, E., Hikita, H., and Ferdous, D., 2003 "Catalytic gasification of sawdust derived from various biomass", *Energy & Fuels* 17, p1456-1463.

Desai, M., Brown, F., Chamberland, B., Jalan, V., 1990 "Copper based sorbent for hot gas cleanup", *Am Chem Soc, Div Fuel Chem* 35, p87-94.

Devi, L., Ptasinski, K. J., and Janssen, F., 2003 "A review of the primary measures for tar elimination in biomass gasification processes", *Biomass & Bioenergy* 24, p125-140.

Elliott, D. C., Neuenschwander, G. G., Hart, T. R., Butner, R. S., Zacher, A. H., Engelhard, M. H., Young, J. S., and McCready, D. E., 2004 "Chemical processing in high-pressure aqueous environments. 7. Process development for catalytic gasification of wet biomass feedstocks", *Industrial & Engineering Chemistry Research* 43, p1999-2004.

Ferreira-Aparicio, P., Benito, M. J., and Sanz, J. L., 2005 "New trends in reforming technologies: from hydrogen industrial plants to multifuel microreformers", *Catalysis Reviews-Science and Engineering* 47, p491-588.

Flytzani-Stephanopoulos, M., Sakbodin, M., and Wang, Z., 2006 "Regenerative adsorption and removal of H2S from hot fuel gas streams by rare earth oxides", *Science* 312, p1508-1510.

Furusawa, T., Miura, Y., Kori, Y., Sato, M., and Suzuki, N., 2009 "The cycle usage test of Ni/MgO catalyst for the steam reforming of naphthalene/benzene as model tar compounds of biomass gasification", Catalysis *Communications* 10, p552-556.

Furusawa, T., and Tsutsumi, A., 2005 “Comparison of Co/MgO and Ni/MgO catalysts for the steam reforming of naphthalene as a model compound of tar derived from biomass gasification”, *Applied Catalysis a-General* 278, p207-212.

Fushimi, C., Araki, K., Yamaguchi, Y., and Tsutsumi, A., 2003 “Effect of heating rate on steam gasification of biomass. 1. Reactivity of char”, *Industrial & Engineering Chemistry Research* 42, p3922-3928.

Garcia, E., Palacios, J. M., Alonso, L., and Moliner, R., 2000 “Performance of Mn and Cn mixed oxides as regenerable sorbents for hot coal gas desulfurization”, *Energy & Fuels* 14, p1296-1303.

Garcia, L., Benedicto, A., Romeo, E., Salvador, M. L., Arauzo, J., and Bilbao, R., 2002 “Hydrogen production by steam gasification of biomass using Ni-Al coprecipitated catalysts promoted with magnesium”, *Energy & Fuels* 16, p1222-1230.

Garcia, T., Solsona, B., and Taylor, S. H., 2006 “Naphthalene total oxidation over metal oxide catalysts”, *Applied Catalysis B-Environmental* 66, p92-99.

Gil, J., Corella, J., Aznar, M. P., and Caballero, M. A., 1999 “Biomass gasification in atmospheric and bubbling fluidized bed: Effect of the type of gasifying agent on the product distribution”, *Biomass & Bioenergy* 17, p389-403.

Hepola, J., and Simell, P., 1997 “Sulphur poisoning of nickel-based hot gas cleaning catalysts in synthetic gasification gas - I. Effect of different process parameters”, *Applied Catalysis B-Environmental* 14, p287-303.

Hepola, J., and Simell, P., 1997 “Sulphur poisoning of nickel-based hot gas cleaning catalysts in synthetic gasification gas - II. Chemisorption of hydrogen sulphide”, *Applied Catalysis B-Environmental* 14, p305-321.

Huang, T. J., and Yu, T. C., 2005 “Effect of steam and carbon dioxide pretreatments on methane decomposition and carbon gasification over doped-ceria supported nickel catalyst”, *Catalysis Letters* 102, p175-181.

Jeong, S. K., Park, T. S., and Hong, S. C., 2001 “Simultaneous SOx/NOx removal in a fluidized bed reactor using natural manganese ore”, *Journal of Chemical Technology and Biotechnology* 76, p1080-1084.

Juutilainen, S. J., Simell, P. A., and Krause, A. O. I., 2006 “Zirconia: Selective oxidation catalyst for removal of tar and ammonia from biomass gasification gas”, *Applied Catalysis B-Environmental* 62, 86-92.

Kalakota, V. R., 2008 “Sulfur removal using regenerable sorbents of rare earth / transition metal oxides” Thesis submitted to the Louisiana State University and Agricultural and Mechanical college.

Kinoshita, C. M., Wang, Y., and Zhou, J., 1994 “Tar formation under different biomass gasification conditions”, *Journal of Analytical and Applied Pyrolysis* 29, p169-181.

Kruse, A., and Gawlik, A., 2003 “Biomass conversion in water at 330-410 degrees C and 30-50 MPa. Identification of key compounds for indicating different chemical reaction pathways”, *Industrial & Engineering Chemistry Research* 42, p267-279.

Kruse, A., Krupka, A., Schwarzkopf, V., Gamard, C., and Henningsen, T., 2005 “Influence of proteins on the hydrothermal gasification and liquefaction of biomass. 1. Comparison of different feedstocks”, *Industrial & Engineering Chemistry Research* 44, p3013-3020.

Kruse, A., Meier, D., Rimbrecht, P., and Schacht, M., 2000 “Gasification of pyrocatechol in supercritical water in the presence of potassium hydroxide”, p4842-4848.

Lamacz, A., Krzton, A., Musi, A., and Da Costa, P., 2009 “Reforming of Model Gasification Tar Compounds”, *Catalysis Letters* 128, p40-48.

Li, K. T., and Chi, Z. H., 2001 “Selective oxidation of hydrogen sulfide on rare earth orthovanadates and magnesium vanadates”, *Applied Catalysis A - General* 206, p197-203.

Li, K. T., Huang, M. Y., and Cheng, W. D., 1996 “Vanadium-based mixed-oxide catalysts for selective oxidation of hydrogen sulfide to sulfur”, *Industrial & Engineering Chemistry Research* 35, p621-626.

Liang, B., Korbee, R., Gerritsen, A. W., and van den Bleek, C. M., 1999 “Effect of manganese content on the properties of high temperature regenerative H2S acceptor”, *Fuel* 78, p319-325.

Li, P. M., Yuan, Z. H., Wu, C. Z., Ma, L. L., Chen, Y., and Tsubaki, N., 2007 “Bio-syngas production from biomass catalytic gasification”, *Energy Conversion and Management* 48, p1132-1139.

Ma, L., Verelst, H., and Baron, G. V., 2005 “Integrated high temperature gas cleaning: Tar removal in biomass gasification with a catalytic filter”, *Catalysis Today* 105, p729-734.

Mastellone, M. L., and Arena, U., 2008 “Olivine as a tar removal catalyst during fluidized bed gasification of plastic waste”, *AIChE Journal* 54, p1656-1667.

Murugan, B and Ramaswamy, A.V., 2005 " Nature of manganese species in Ce1-*x*Mn*x*O2-*ä* solid solutions synthesized by the solution combustion route", *Chem. Mater* 17, p3983-3993 3983.

Milne, T.A., Elam, C.C., Evans, R.J., 2003 " Hydrogen from biomass: state of the art and research challenges", *Report to International Energy Agency*, IEA/H2/TR-02/01.

Nacken, M., Ma, L., Engelen, K., Heidenreich, S., and Baron, G. V., 2007 "Development of a tar reforming catalyst for integration in a ceramic filter element and use in hot gas cleaning", *Industrial & Engineering Chemistry Research* 46, 1945-1951.

Narvaez, I., Corella, J., and Orio, A., 1997 "Fresh tar (from a biomass gasifier) elimination over a commercial steam-reformimg catalyst. Kinetics and effect of different variables of operation", *Industrial & Engineering Chemistry* Research 36, p317-327.

Neeft, J., Knoef, H., Zielke, U., SjÖstrÖm, K., Hasler, P., SimellI, P., Dorrington, M., Thomas, L., Abatzoglou, N., Deutch, S., Greil, C., Buffinga, G., Brage, C. & Suomalainen, M., "Guidelines for Sampling and Analysis of Tar and Particles in Biomass Producer Gases" *Progress in thermochemical biomass conversion*, A.V. Bridgewater, ed., Blackwell Science, London, 2001, Chapter11, p162-175.

Ozawa, M., and Loong, C. K., 1999 "In situ X-ray and neutron powder diffraction studies of redox behavior in CeO2-containing oxide catalysts", *Catalysis Today* 50, p329-342.

Pansare, S. S., Goodwin, J. G., and Gangwal, S., 2008 "Simultaneous Ammonia and Toluene Decomposition on Tungsten-Based Catalysts for Hot Gas Cleanup", *Industrial & Engineering Chemistry Research* 47, p8602-8611.

Pengpanich, S., Meeyoo, V., Rirksomboon, T., and Bunyakiat, K., 2002 "Catalytic oxidation of methane over CeO2-ZrO2 mixed oxide solid solution catalysts prepared via urea hydrolysis", *Applied Catalysis A - General* 234, p221-233.

Pengpanich, S., Meeyoo, V., Rirksomboon, T., and Schwank, J., 2006 "Hydrogen production from partial oxidation of iso-octane over Ni/Ce0.75Zr0.25O2 and Ni/beta "-Al2O3 catalysts", *Applied Catalysis A - General* 302, p133-139.

Raman, K. P., Walawender, W. P., and Fan, L. T., 1980 "Gasification of feedlot manure in a fluidized-bed reactor - the effect of temperature", *Industrial & Engineering Chemistry Process Design and Development* 19, p623-629.

Ramirez-Cabrera, E., Laosiripojana, N., Atkinson, A., and Chadwick, D., 2003 "Methane conversion over Nb-doped ceria", p433-438.

Rapagna, S., Jand, N., and Foscolo, P. U., 1998 “Catalytic gasification of biomass to produce hydrogen rich gas”, *International Journal of Hydrogen Energy* 23, p551-557.

Rapagna, S., Jand, N., Kiennemann, A., and Foscolo, P. U., 2000 “Steam-gasification of biomass in a fluidised-bed of olivine particles”, *Biomass & Bioenergy* 19, p187-197.

Sato, K., and FujiMoto, K., 2007 “Development of new nickel based catalyst for tar reforming with superior resistance to sulfur poisoning and coking in biomass gasification”, *Catalysis Communications* 8, p1697-1701.

Sato, K., Shinoda, T., and Fujimoto, K., 2007 “New nickel-based catalyst for tar reforming, with superior resistance to coking and sulfur poisoning in biomass gasification processes”, *Journal of Chemical Engineering of Japan* 40, p860-868.

Schmersahl, R., Mumme, J., and Scholz, V., 2007 “Farm-based biogas production, processing, and use in polymer electrolyte membrane (PEM) fuel cells”, *Industrial & Engineering Chemistry Research* 46, p8946-8950.

Schmieder, H., Abeln, J., Boukis, N., Dinjus, E., Kruse, A., Kluth, M., Petrich, G., Sadri, E., and Schacht, M., 2000 “Hydrothermal gasification of biomass and organic wastes”, *Journal of Supercritical Fluids* 17, 145-153.

Simell, P. A., and Bredenberg, J. B., 1990 “Catalytic purification of tarry fuel gas”, *Fuel* 69, p1219-1225.

Simell, P. A., Leppalahti, J. K., and Bredenberg, J. B. S., 1992 “Catalytic purification of tarry fuel gas with carbonate rocks and ferrous materials”, *Fuel* 71, p211-218.

Swierczynski, D., Courson, C., Bedel, L., Kiennemann, A., and Guille, J., 2006 “Characterization of Ni-Fe/MgO/olivine catalyst for fluidized bed steam gasification of biomass”, *Chemistry of Materials* 18, p4025-4032.

Tasaka, K., Furusawa, T., and Tsutsumi, A., 2007 “Biomass gasification in fluidized bed reactor with Co catalyst”, p5558-5563.

Tasaka, K., Furusawa, T., and Tsutsumi, A., 2007 “Steam gasification of cellulose with cobalt catalysts in a fluidized bed reactor”, *Energy & Fuels* 21, p590-595.

Terorde, R., Vandenbrink, P. J., Visser, L. M., Vandillen, A. J., and Geus, J. W., 1993 “Selective oxidation of hydrogen-sulfide to elemental sulfur using iron-oxide catalysts on various supports”, p217-224.

Torres, W., Pansare, S. S., and Goodwin, J. G., 2007 “Hot gas removal of tars, ammonia, and hydrogen sulfide from Biomass gasification gas”, *Catalysis Reviews-Science and Engineering* 49, p407-456.

Turn, S. Q., 2007 “Chemical equilibrium prediction of potassium, sodium, and chlorine concentrations in the product gas from biomass gasification”, *Industrial & Engineering Chemistry Research* 46, p8928-8937.

Wakker, J. P., Gerritsen, A. W., and Moulijn, J. A., 1993 “High-temperature H2S and COS removal with MnO and FeO on gamma-Al2O3 acceptors”, *Industrial & Engineering Chemistry Research* 32, p139-149.

Waldner, M. H., and Vogel, F., 2005 “Renewable production of methane from woody biomass by catalytic hydrothermal gasification”, *Industrial & Engineering Chemistry Research* 44, p4543-4551.

Wang, Z., and Flytzani-Stephanopoulos, M., 2005 “Cerium oxide-based sorbents for regenerative hot reformate gas desulfurization”, *Energy & Fuels* 19, p2089-2097.

Wen, W. Y., and Cain, E., 1984 “Catalytic pyrolysis of a coal-tar in a fixed-bed reactor”, *Industrial & Engineering Chemistry Process Design and Development* 23, p627-637.

Westmoreland, P. R., Gibson, J. B., and Harrison, D. P., 1977 “Comparative kinetics of high-temperature reaction between h2s and selected metal-oxides”, *Environmental Science & Technology* 11, p488-491.

Yamaguchi, Y., Fushimi, C., Tasaka, K., Furusawa, T., and Tsutsumi, A., 2006 “Kinetic study on the pyrolysis of cellulose using the novel continuous cross-flow moving bed type differential reactor”, *Energy and Fuels* 20, p2681-2685.

Yasyerli, S., 2008 “Cerium–manganese mixed oxides for high temperature H2S removal and activity comparisons with V–Mn, Zn–Mn, Fe–Mn sorbents”, *Chemical Engineering and Processing*, 47, p577–584.

Yoon, Y. I., Kim, M. W., Yoon, Y. S., and Kim, S. H., 2003 “A kinetic study on medium temperature desulfurization using a natural manganese ore”, *Chemical Engineering Science* 58, p2079-2087.

Zeng, Y., Zhang, S., Groves, F. R., and Harrison, D. P., 1999 “High temperature gas desulfurization with elemental sulfur production”, *Chemical Engineering Science* 54, p3007-3017.

Zhang, R. Q., Cummer, K., Suby, A., and Brown, R. C., 2005 “Biomass-derived hydrogen from an air-blown gasifier”, *Fuel Processing Technology* 86, p861-874.

APPENDIX A - GAS CHROMATOGRAPHY DETAILS

A.1 Naphthalene cracking

Table A.1. 1 GC settings for naphthalene cracking analysis

Parameter	Setting
Column Oven temperature	423K
Detector (FID) temperature	433K
Injection port temperature	473K
Sampling valve temperature	403K
Column	J&W DB-5, 1.5 micron film, 30 m x 0.53mm
Carrier gas	He, 12 mL/min
Auxiliary ga	He, 15 mL/min
Hydrogen flow	35 mL/min
Air flow	340 mL/min
Split flow	He, 20 mL/min
Septum purge flow	He, 2.5 mL/min
Range	2
Attenuation	0

The FID (flame ionization detector) for the HP 5890 Series II GC was calibrated for naphthalene by injecting naphthalene dissolved in heptane solution. 0.02 mol/L of Naphthalene in Heptane solution was prepared. Either 0.2, 0.5, or 1 µL of this solution were injected and the samples were analysed as in Table A.1.2 with results in Figure A.1.

Table A.1. 2 Temperature program for manual injections

Initial time	1 min
Initial temperature	373 K
Final temperature	423 K
Ramp	5 K/min
Final time	1 min

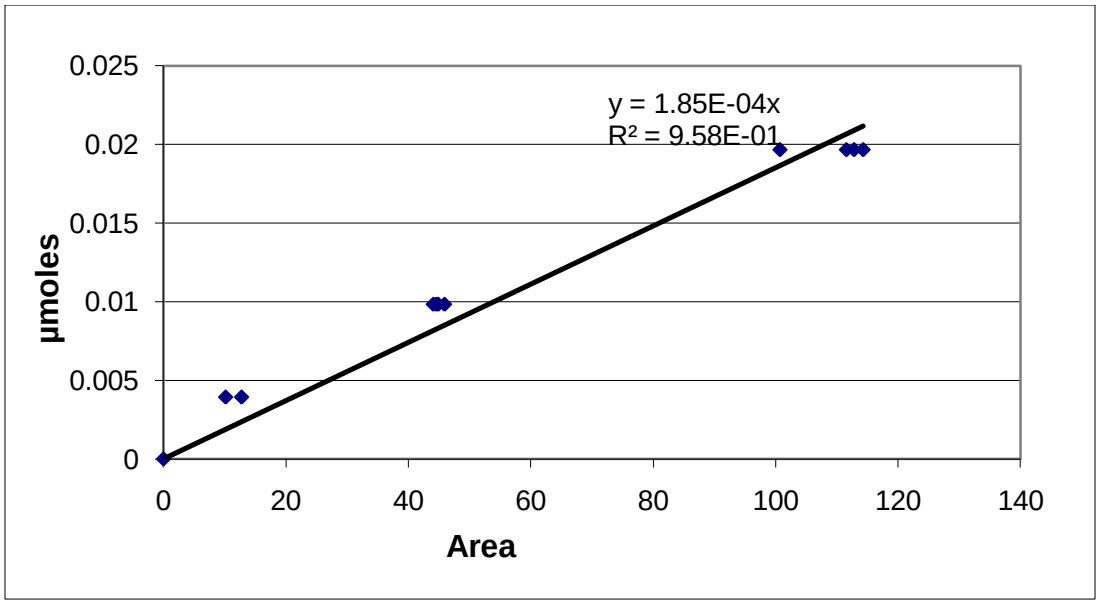

Figure A. 1 Naphthalene calibration

The response factor for naphthalene was calculated as:

$$RF_{naph} = X_{naph} / Area_{naph}$$

Where X_{naph} is micromoles of naphthalene. The response factor was 1.85×10^{-4} µmol/area unit with an R^2 of 0.958.

A.2. Sulfur compound analysis

For this analysis, a Varian 3800 GC was used. It was equipped with a pulsed flame photometric detector (PFPD) which is specific for sulfur compounds down to sulfur concentrations of ~1 ppmv.

Table A.2. 1 GC settings for product analysis

Parameter	**Setting**
Column Oven temperature	373K
Sampling valve temperature	373K
PFPD detector temperature	473K
TCD detector temperature	473K

Table A.2. 2 Varian 3800 settings for sulphur compound analysis

Column	0.53 mm capillary, no stationary phase
Carrier gas	He, 15mL/min
Air 1	34 mL/min
Air 2	10 mL/min
Hydrogen	20 mL/min
PFPD Range	9.0
PFPD Photomultiplier voltage	630 V
PFPD Gate width	20 ms
PFPD Gate delay	6.0 ms
PFPD Trigger level	220 mV
Sample loop size	2 mL

The PFPD was calibrated using 1% H_2S/N_2 and CO_2 mixtures; three samples were averaged for each mixture. The response factor (RF) for PFPD was calculated :

$$RF = X_{H2S} / A_{H2S}$$

Where X_{H2S} is micromoles of H_2S. The response factor was 0.339 µmole/area unit and the results are in Figure A.2.

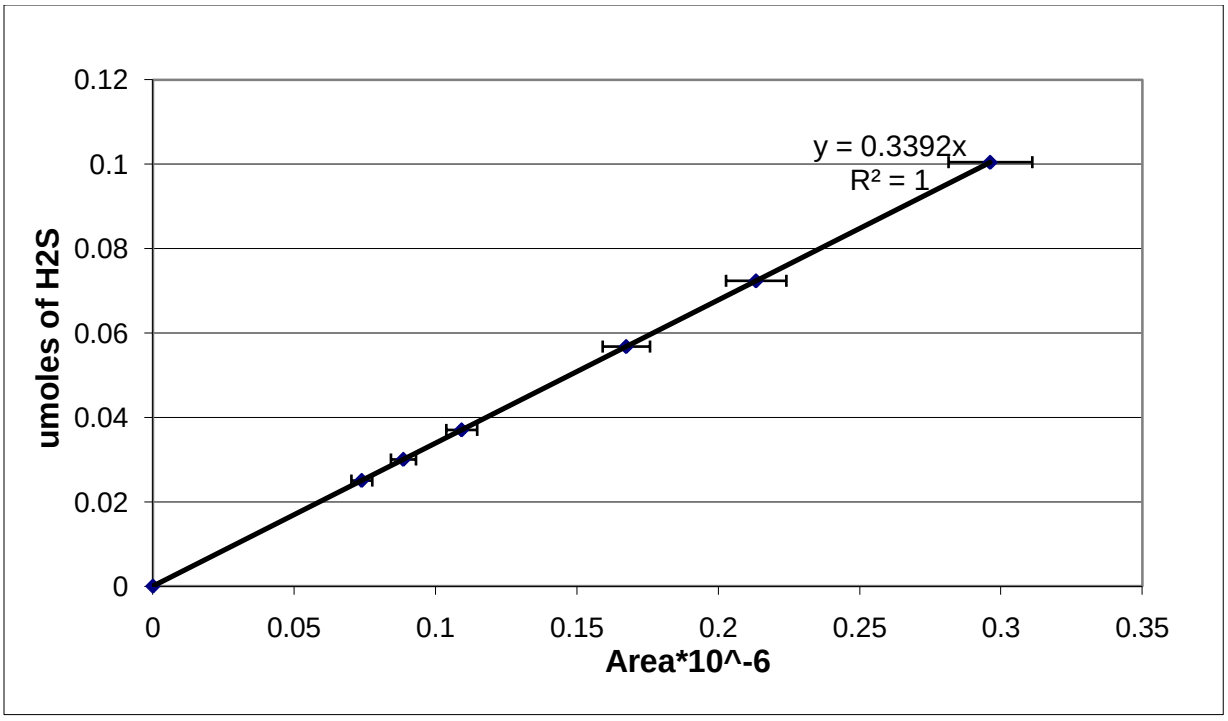

Figure A. 2 Calibration for H_2S

VITA

Sumana Adusumilli was born in December 1985, to Jyothi and Lakshmana Rao Adusumilli, in Tenali, Andhra Pradesh, India. She completed her college studies in Vijayawada in 2003. She then joined the Department of Chemical Engineering at Andhra University and earned a Bachelor of Technology in 2007. In August 2007, she was admitted to Louisiana State University, Chemical Engineering Department. There she worked under Dr. Kerry M. Dooley and completed her research work successfully in December 2009. This thesis completes her requirements to receive the degree of Master of Science in Chemical Engineering.